

University of New Hampshire

University of New Hampshire Scholars' Repository

Doctoral Dissertations

Student Scholarship

Fall 1997

An analysis of high frequency methane measurements in central New England

Mark Charles Shipham
University of New Hampshire, Durham

Follow this and additional works at: <https://scholars.unh.edu/dissertation>

Recommended Citation

Shipham, Mark Charles, "An analysis of high frequency methane measurements in central New England" (1997). *Doctoral Dissertations*. 1982.
<https://scholars.unh.edu/dissertation/1982>

This Dissertation is brought to you for free and open access by the Student Scholarship at University of New Hampshire Scholars' Repository. It has been accepted for inclusion in Doctoral Dissertations by an authorized administrator of University of New Hampshire Scholars' Repository. For more information, please contact Scholarly.Communication@unh.edu.

INFORMATION TO USERS

This manuscript has been reproduced from the microfilm master. UMI films the text directly from the original or copy submitted. Thus, some thesis and dissertation copies are in typewriter face, while others may be from any type of computer printer.

The quality of this reproduction is dependent upon the quality of the copy submitted. Broken or indistinct print, colored or poor quality illustrations and photographs, print bleedthrough, substandard margins, and improper alignment can adversely affect reproduction.

In the unlikely event that the author did not send UMI a complete manuscript and there are missing pages, these will be noted. Also, if unauthorized copyright material had to be removed, a note will indicate the deletion.

Oversize materials (e.g., maps, drawings, charts) are reproduced by sectioning the original, beginning at the upper left-hand corner and continuing from left to right in equal sections with small overlaps. Each original is also photographed in one exposure and is included in reduced form at the back of the book.

Photographs included in the original manuscript have been reproduced xerographically in this copy. Higher quality 6" x 9" black and white photographic prints are available for any photographs or illustrations appearing in this copy for an additional charge. Contact UMI directly to order.

UMI

**A Bell & Howell Information Company
300 North Zeeb Road, Ann Arbor MI 48106-1346 USA
313/761-4700 800/521-0600**

**AN ANALYSIS OF HIGH FREQUENCY METHANE MEASUREMENTS IN CENTRAL
NEW ENGLAND**

BY

MARK C. SHIPHAM
B.S., North Carolina State University, 1980
M.S., North Carolina State University, 1984

DISSERTATION

**Submitted to the University of New Hampshire
in Partial Fulfillment of
the Requirements for the Degree of**

Doctor of Philosophy

in

Earth Sciences

September, 1997

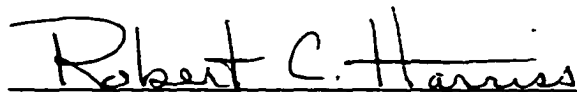
UMI Number: 9807567

UMI Microform 9807567
Copyright 1997, by UMI Company. All rights reserved.

**This microform edition is protected against unauthorized
copying under Title 17, United States Code.**

UMI
300 North Zeeb Road
Ann Arbor, MI 48103

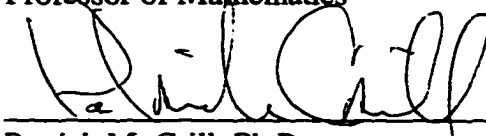
This dissertation has been examined and approved.



Dissertation Director, Robert C. Harriss, Ph.D.
Professor of Earth Sciences



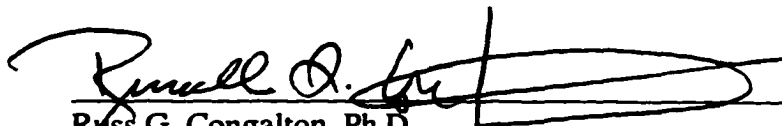
L. D. Meeker, Ph.D.
Professor of Mathematics



Patrick M. Crill, Ph.D.
Research Associate Professor of Earth Sciences



J. William Munger, Ph.D.
Research Associate of Atmospheric Chemistry



Russ G. Congalton, Ph.D.
Associate Professor of Remote Sensing and GIS



Karen Bartlett, M.S.
Research Scientist

20 JUNE 1997

Date

ACKNOWLEDGMENTS

This work would not have been possible without the counsel and assistance of many people. I would like to thank NASA and in particular all the folks in the Atmospheric Sciences Division in which I work for all their support and efforts on my behalf. I deeply appreciate the guidance and advice from all of my committee members. As always it has been a pleasure to work with Dr. Robert Harriss whom I have the utmost respect for. His optimistic outlook and great enthusiasm helped me to keep pushing on when at times I certainly did not feel like it. Thanks to Karen Bartlett for her many readings of the rough drafts and all of her good ideas and insight. Thanks to Dave Meeker for his time and patience and the use of his data analysis software which was invaluable. Thanks to Bill Munger for keeping me straight on the Harvard Forest data sets and his many good ideas.

I would like to thank my family and many friends who had to listen to my complaints when to going got tough. In particular my mother, Eileen S. Huff, who I think worried more than I as I progressed through all the trial and tribulations in pursuit of this degree.

TABLE OF CONTENTS

	Page
ACKNOWLEDGMENTS	iii
TABLE OF CONTENTS	iv
LIST OF TABLES	vi
LIST OF FIGURES	vii
ABSTRACT	x
Chapter	
I. INTRODUCTION AND GOALS	1
II. BACKGROUND	3
III. SITE DESCRIPTION AND INSTRUMENT METHODOLOGY	5
IV. DATA ANALYSIS METHODS	8
V. LONG TERM TREND, SEASONAL, AND DIURNAL CYCLES	13
Long term trend	13
Seasonal cycles	16
Diurnal cycles	19
VI. POLLUTION EPISODES AT THE HARVARD FOREST SITE	28
Location of Sources	28
Characterizing the Harvard Forest flow regime	32
Wind Direction and Speed	34
Methane Enhancements	36
Acetylene Enhancements	38

Summer Hexane and 1,3-Butadiene Enhancements	39
Correlations between Methane and Acetylene	41
Summer Correlations between Methane and Short Lived Species	42
VII. THE CHEMICAL SIGNATURE OF THE HF REGION.....	44
The High Emissions Sector	44
The Clean Air Sector	45
Worcester, MA. and Providence, RI.....	48
Boston, MA.....	49
Petersham, MA.....	51
Site Sensitivities.....	52
Yearly Changes in the HES and CAS	53
VIII. CASE STUDIES	57
Criteria / Grouping.....	57
Case study 1: 17- 20 February, 1994.....	58
Case study 2: 13-14 January 1995.....	60
Case study 3: 6 August 1992.....	62
IX. CONCLUSIONS	65
APPENDIX A: POSSIBLE SOURCES OF ERROR	68
LIST OF REFERENCES	72

LIST OF TABLES

I.	Monthly and Seasonal Summary Statistics of Methane for 1992	14
II.	Monthly and Seasonal Summary Statistics of Methane for 1993	15
III.	Monthly and Seasonal Summary Statistics of Methane for 1994	16
IV.	Monthly and Seasonal Summary Statistics of Methane for 1995	17
V.	Heading, Distance, and Populations of Selected Cities in the Region.....	29
VI.	Heading and Distance to Regional Landfills.	31
VII.	Primary Sources and Estimated Lifetimes* for Selected NMHC's.....	33
VIII.	Mean and Standard Deviation for Selected Wind Quadrants	45
IX.	Yearly Summary Statistics for the CAS and HES.....	54
X.	Sources of Potential Error	71

LIST OF FIGURES

Figure 1: Frequency distribution of methane mixing ratios for (a) January and (b) July 1993. Solid lines bracket the lower 10 to 30% of the data range. Both high and occasional low events are separated from the background data.	9
Figure 2: Concentrations of methane for the global CMDL network and Harvard Forest. X's are the mean with bar length being ± 1 standard deviation.	10
Figure 3: Least-squares frequency analysis of methane mixing ratios at Harvard Forest for 1992-1995.	11
Figure 4: The atmospheric mixing ratios of methane at Harvard Forest between 1992 and 1995. These data show a variable upward trend, seasonal cycles, and the many pollution events that affect the site.	18
Figure 5: Monthly median and median absolute deviation of mixing ratios of methane for 1992-1995. The X's (all data) and O's (background data) represent the median mixing ratios overlaid by an error bar of ± 1 median absolute deviation. The curves are generated by robust spline fitting algorithm using the monthly data.	19
Figure 6: Background data seasonal cycles for 1992 - 1995. Symbols for each year are the monthly mean mixing ratios. Curves are generated by a robust spline fit algorithm. .	20
Figure 7: Full data set seasonal cycles for 1992-1995.....	21
Figure 8: Residuals representing the monthly means of the full minus monthly means of the background data. The residuals are largest in the winter and smallest in the summer.	22
Figure 9: Mean diurnal cycle observed for each month, December-November (a-l). Number in the lower left hand corner is maximum-minimum mixing ratio.	24
Figure 10: The mean diurnal cycle for March, April, and May, 1993.....	26
Figure 11: The mean diurnal cycle for July, August, and September, 1993.	27
Figure 12: Regional cities and major highways surrounding Harvard Forest (X). Note the location of Springfield, MA. and New York, NY. to the southwest, Boston, MA. to the east, and Providence, RI. to the southeast.	28

Figure 13: Landfills surrounding Harvard Forest (*). The strongest sources closest to HF are located at Peabody, MA. to the east and East Bridgewater and Plainville, MA. to the southeast. Note the nearby cluster of landfills to the southwest of the site. (Figure courtesy Blaha et al., in press.)	30
Figure 14: Wind direction (%), (a-c) and speed (m/s) (d-f) at the Harvard Forest tower for annual, winter, and summer time periods.	35
Figure 15: Enhanced methane mixing ratios for (a) annual, (b) winter, (c) summer and, (d) winter-summer time periods.	37
Figure 16: Enhanced acetylene mixing ratios for (a) annual, (b) winter, and (c) summer time periods.	38
Figure 17: Summer enhanced (a) hexane and (b) 1,3-butadiene mixing ratios.	40
Figure 18: Correlation coefficients between methane and acetylene for (a) annual, (b) winter, and (c) summer time periods.	41
Figure 19: Summer correlations between (a) methane and hexane and (b) methane and 1,3-butadiene.	43
Figure 20: Methane plotted as a function of (a) acetylene, (b) hexane, (c) propane, and (d) ethane for the HES. Correlations between species are shown in the upper left of each figure. Data is fit by a least-squares algorithm.	46
Figure 21: Methane plotted as a function of (a) acetylene, (b) hexane, (c) propane, and (d) ethane for the CAS.	47
Figure 22: Methane plotted as a function of (a) acetylene, (b) hexane, (c) propane, and (d) ethane for Worcester, MA and Providence, RI.	49
Figure 23: Methane plotted as a function of (a) acetylene, (b) hexane, (c) propane, and (d) ethane for Boston, MA.	50
Figure 24: Methane plotted as a function of (a) acetylene, (b) hexane, (c) propane, and (d) ethane for Petersham, MA.	51
Figure 25: Winter methane and acetylene for the HES and CAS for years 1993 - 1995 (a-d). The cross bars are the mean and ± 1 standard deviation for each species as a function of season.	55
Figure 26: Summer methane and acetylene for the HES and CAS for years 1992 - 1995 (a-d).	56

Figure 27: Methane, acetylene, hexane, ratio of pentane and ethane, wind direction, and speed for 17-20 February, 1994.....	59
Figure 28: Methane, acetylene, hexane, ratio of pentane and ethane, wind direction, and speed for 13-14 January, 1995.....	61
Figure 29: Methane, acetylene, hexane, ratio of pentane and ethane, wind direction, and speed for 6 August 1992.	63

ABSTRACT

AN ANALYSIS OF HIGH FREQUENCY METHANE MEASUREMENTS IN CENTRAL NEW ENGLAND

BY

MARK C. SHIPHAM

University of New Hampshire, September, 1997

A unique high resolution ambient air methane data set consisting of approximately 125,000 independently measured data points for the years 1991-1995 has been collected at a site in the northeastern United States. This data base is used to examine the long term trend, seasonal and diurnal cycles, and the frequent pollution events that affect the site on a year round basis.

The annual median mixing ratio of methane for all measurements was 1808 ppbv in 1992, increasing at a variable rate to 1837 ppbv in 1995. The lower 10-30% of the data from each month was defined as representative of background air and was compared to the global CMDL data set. The background data exhibit a variable upward trend of 5.5 ± 2 ppbv/year during the 4-year time period, with most of the increase observed during 1993 and 1994.

The seasonal cycle for the background data set is similar to what is observed by CMDL stations and varies from 24 to 35 ppbv. The amplitude of the seasonal cycle for the full data set was larger, ranging from 35 to 44 ppbv. Differences between the full and background mixing ratios vary on a seasonal basis and are largest in the winter and small-

est in the summer. These differences appear to be controlled by changes in atmospheric stability and changes in emissions from local and regional sources throughout the year.

Wind roses of chemical species are examined for annual and seasonal time periods with enhancements in anthropogenic species corresponding to the location of large cities and landfills. Methane is strongly correlated to species that have an anthropogenic component, including acetylene, propane, ethane, and hexane. The southwest quadrant is subjected to the most severe pollution events and is impacted by outflow from large cities in that sector, including Northampton and Springfield, MA. Emissions from cities in other quadrants, including Boston and Worcester, MA., Providence, RI., and the near by town of Petersham, MA. also affect the site, but to a lesser degree.

Case studies are used to identify atmospheric conditions that lead to high concentrations of methane and other species. The co-occurrence of a persistent wind direction, light wind speed, and stable atmospheric conditions is the ideal scenario in which emissions from nearby cities and landfills are advected to the site. Emissions from local and regional, rather than distant sources, are the primary cause of elevated events.

CHAPTER I

INTRODUCTION AND GOALS

In 1993 the United States released a climate action plan proposing to return U.S. greenhouse gas emissions to the 1990 level by the year 2000. The largest contributor to the potential of global warming is carbon dioxide (CO_2), followed by methane (CH_4). Stabilizing the atmospheric burden of CO_2 will require a reduction in emissions of 60-80%. This is unlikely in the near future given industrial societies strong dependence on fuels coupled with the 200 year life time of CO_2 . In comparison, CH_4 emissions need to be reduced only 10 to 15% to stabilize its global concentration and the 11 year life time of CH_4 means the affects of mitigation strategies may be observed within several decades.

A critical factor in determining if mitigation strategies are working is the paucity of quantitative measurements of CH_4 at local to regional scales in which changes in emissions over long time periods may be verified. To address this problem automated high-frequency (8-11 minute) CH_4 measurements have been made by Dr. Patrick M. Crill from the University of New Hampshire at the Harvard forest (HF) research site since 1992. The proximity of this site to numerous industrial/urban areas presents the opportunity to sample from known CH_4 sources on a regular and repeatable basis and to characterize the chemical signature of the sampling location and assess its sensitivity to both local and regional sources.

The first section of this dissertation examines the long-term trend and seasonal and diurnal cycles of CH_4 at the HF research site. Key questions that are addressed include:

How does the long term trend at this site, which is located in an heavily industrialized region, compare to the observed trends for clean air sites in the Northern hemisphere?
How is the timing and amplitude of the seasonal cycle altered by air pollution events?
What is the amplitude and timing of the daily cycle and how does it relate to changes in local sources of CH₄, atmospheric stability, and solar input.

The second section characterizes the effects of air pollution in the HF region through the use of additional chemical species and meteorological parameters. Key questions that are examined include: Can the effects of local, regional, and distant CH₄ sources be quantified? Can annual and seasonal enhancements of chemical species be related to emissions from sources in particular wind sectors? Are the frequency and severity of pollution events changing over time? Can individual sources of pollutants be identified on a regular basis?

Over a longer time frame this data set will be used to determine if the mitigation strategies for CH₄ are working. This first four years of data provides an invaluable benchmark in understanding the regional behavior of CH₄ and will become part of a much larger multi-year data set that will hopefully one day reveal that regional CH₄ concentrations are stabilizing or even declining as the effects of reduction strategies take hold.

CHAPTER II

BACKGROUND

A series of reports by the Intergovernmental Panel on Climate Change [*IPCC, 1990, 1992, 1995*] provides a comprehensive assessment of global sources and sinks of atmospheric CH₄. Individual articles and references contained in the IPCC documents suggest that human activities are now responsible for approximately 70% of the global CH₄ sources. Anthropogenic inputs of CH₄ are associated with energy production and use, landfills, domestic sewage, rice agriculture, domestic ruminants, and animal wastes. Natural sources include wetlands, termites, lakes, and coastal waters.

Future growth in CH₄ sources has been estimated by the IPCC, with the largest growth expected to occur in emissions from landfills, energy production and use, and from animal production/waste systems. Sources with modest expected growth are biomass burning and rice agriculture. In the United States the largest anthropogenic sources of CH₄ are from landfills which account for about 25% of total emissions [*EPA, 1994*].

While the yearly rate of increase in the mixing ratios of CH₄ is variable [*Steele et al., 1992; Harris et al., 1992; Khalil et al., 1993A; Conway et al., 1994; Dlugokencky et al., 1994A; and Keeling et al., 1995*], over the past two centuries they have approximately doubled [*Etheridge et al., 1992; Thompson et al., 1993; and Khalil et al., 1994*]. On a geologic time scale ice-core records show the current mixing ratios of CH₄ to be two to three times higher than has been observed during the past one hundred and sixty thousand years [*Chappellaz et al., 1990*], with the doubling over the past two centuries representing an

unprecedented rise of CH₄.

Since 1983, CH₄ measurements have been made at approximately weekly time intervals at an increasing number of stations around the globe by the National Oceanic and Atmospheric Administrations's Climate Monitoring and Diagnostic Laboratory (NOAA/CMDL) [*Lang et al., 1990A, 1990B; Steele et al., 1992*]. This extensive world wide network collects background, clean air measurements of CH₄ which provide insight into the complex temporal cycles that compose the changing global CH₄ signal [*Steele et al., 1987; Blake et al., 1988; Conway et al., 1994; Dlugokencky et al., 1994A*].

The Harvard Forest data set is the first multi-year high frequency data collected in a densely populated, heavily industrialized region and will be utilized to examine complex interactions between natural and man made sources and sinks of CH₄.

CHAPTER III

SITE DESCRIPTION AND INSTRUMENT METHODOLOGY

The 1200 ha HF research site is located in Petersham, MA. (42.48° N, -72.18° W; elevation 340 m) is ideally located to sample air from numerous anthropogenic CH₄ sources and is subjected to pollution events on a year round basis. The micrometeorological tower from which the samples are taken is 30 m high and is situated within a 60-year old mixed hardwood forest typical of the transition hardwood-white pine-hemlock forests in much of the region. There is a highway approximately 5 km to the north and a secondary road 2 km to the west. A dirt road leads to the site and has very limited vehicular traffic. Depending on the prevailing wind speed and direction, the instruments on the tower generally sample air with trajectories from industrial/urban environments to the south and southwest and from rural landscapes to the west and north.

The automatic CH₄ analysis system was designed and is maintained by Dr. Patrick M. Crill from the University of New Hampshire and is built around a Shimadzu Mini-2 gas chromatograph equipped with a flame ionization detector. Ambient air is continuously sampled from an inlet 20 m above the ground surface (a few meters above the forest canopy) through 1/4" o.d. plastic coated aluminum tubing (Dekoron 041943-1 tubing) with an electric diaphragm pump at a rate of 25 l/min. This flow is sampled every 8-11 minutes with a Valco stream select valve, dried across a 1 m Perma Pure nafion drier and, after sample loop pressure is allowed to relax to atmospheric pressure, 1 ml is injected into the carrier gas stream of the chromatograph by another Valco electrically-actuated valve. The

sampling procedure yields an independent measurement of ambient CH₄ every 8-11 minutes. CH₄ is separated on a 2 m by 3.2 mm o.d. stainless steel column packed with HayeSep Q at 40° C. Detector temperature is 125° C. Valve timing, analog to digital conversion of the detector output, and signal integration is controlled by a Hewlett-Packard HP3395A series II integrator with an HP19405A event controller. Raw data and integration reports are transferred to and stored on a personal computer until the data are transferred to the University of New Hampshire in Durham, NH via modem every three days.

During operation a field calibration sample is processed with each ambient air sample. The field standard are cylinders of breathing air containing near-ambient mixing ratios of CH₄ that have been calibrated with Niwot Ridge air standards prepared by NOAA/CMDL in Boulder, CO. Over the course of a day, the standard response of the gas chromatograph varies about 1% due to diel heating and cooling since the standard is kept in an unheated pump room in order to mimic the temperature of the outside air sample. Therefore, to evaluate the precision of the CH₄ measurements, the responses of an individual analysis of the standard is compared to the 24-minute running average of the standard response. The coefficient of variation (c.v.; the standard deviation/mean) expressed as the percent variation from the 24-minute running mean ranged annually from 0.18 to 0.29%. If this c.v. represents the sum of errors in the system measurement (an assumption not entirely true since the standard does not flow through the sampling pump) then the precision of the analysis would be considered to 3.6 ± 0.4 ppbv CH₄.

Additionally, all data points were filtered for instrument response by calculating the difference between each standard response and its average with the two points on either side. This difference was then divided by the sample standard deviation for these

same 5 points. The resulting number was then compared to the mixing ratios obtained by the Grubbs test for outliers at a significance level of 95% [Sokal and Rohlf, 1981] and removed if it exceeded that value. No data were removed in 1992 and 1993, 1.4% were removed in 1994, and 1.55% were removed in 1995. Appendix A contains an extended discussion of sources of errors in the data bases.

In addition to CH₄ measurements of many other chemical constituents and meteorological parameters are currently being made at the tower by other researchers [Munger *et al.*, 1996; Goldstein *et al.*, 1995A]. Measurements of fluxes of CO₂, O₃, H₂O, and NO_y and ambient concentrations of CO, CO₂, O₃, H₂O, NO_x, and NO_y are described by Wofsy *et al.* 1993 and Munger *et al.*, 1996 respectively, and for C₂-C₆ by Goldstein *et al.* [1995B].

CHAPTER IV

DATA ANALYSIS METHODS

Analysis of the time series for these data present challenging problems. First, the data must be considered non-uniformly sampled due to variable length data gaps, some of which are several weeks in duration. This precludes standard time series analysis techniques which assume evenly spaced data. Second, the series is a non-stationary process in that the underlying global and regional sources and sinks of CH₄ are changing and changing at different rates over time. As a consequence, robust statistical techniques resistant to outliers are used in the analysis of the full data set [*Meeker et al., 1995; Khalil et al., 1993C; McRae et al., 1979*].

A sub-set of these data is used to examine the long term trend and seasonal cycle in background, clean air conditions comparable to those observed by the global CMDL network. Following work by *Goldstein et al., 1995*, the lower 10-30% of CH₄ mixing ratios from each month are considered to be representative of a background air mass. While the full data set is skewed by pollution events and is non-normally distributed, the lower 10-30% of the data has a near normal frequency distribution as would be expected when extreme values are removed [*Gaines et al., 1993*]. Elimination of the lowest 10% of CH₄ mixing ratios removes low values that may associated with either diluted stratospheric or aged tropical air which is not representative of surface background conditions at the HF site.

The frequency distribution of mixing ratios for January and June, 1993 is shown in

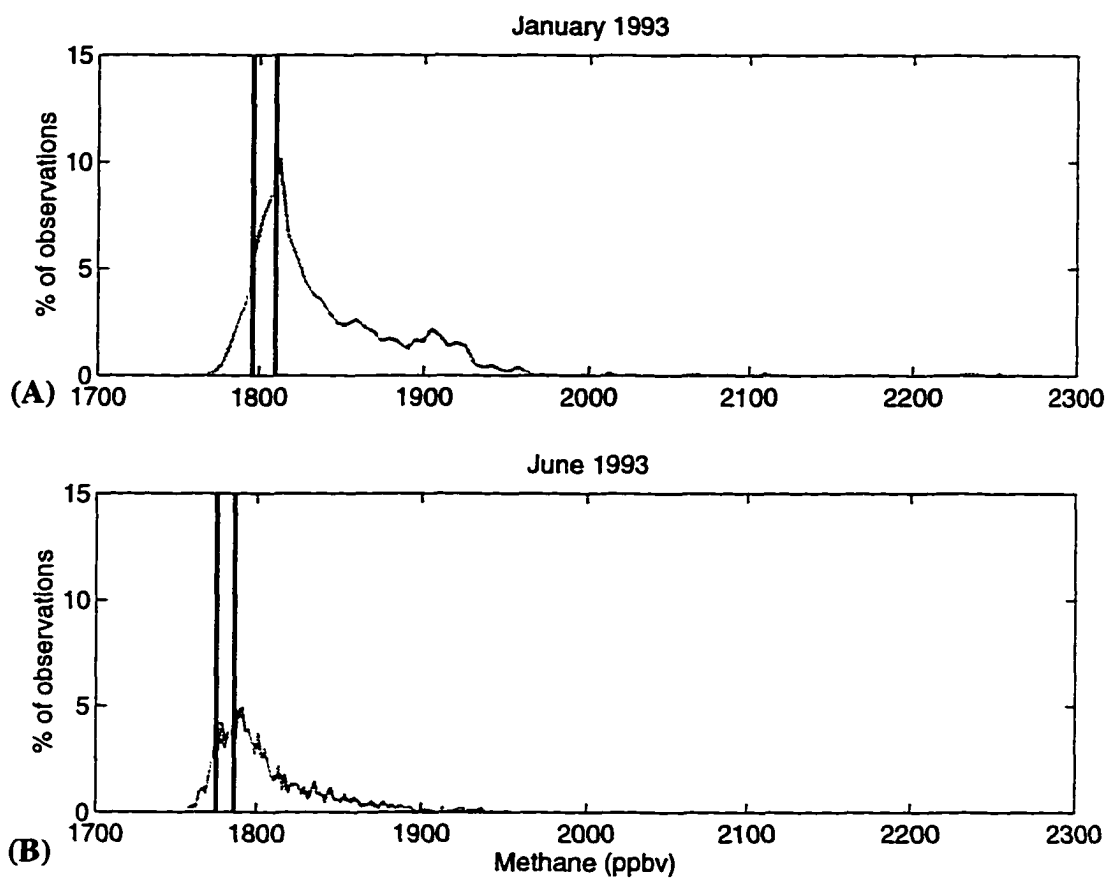


Figure 1: Frequency distribution of methane mixing ratios for (a) January and (b) July 1993. Solid lines bracket the lower 10 to 30% of the data range. Both high and occasional low events are separated from the background data.

Figures 1a and b. In January, the lower 10-30% of mixing ratios range from 1796 to 1810 ppbv, eliminating several severe pollution events that occurred during the month. Likewise, the data envelope for June bounds mixing ratios from 1775 to 1786 ppbv, again eliminating high episodes of CH_4 associated with pollution and/or stagnation events.

The mixing ratio for the HF background data for 1993 is compared to the CMDL data network in Figure 2. The background annual average mixing ratio of 1796 ppbv at HF is similar to CMDL sites near this same latitude. The mean HF mixing ratio using the full database is 1828 ppbv, an enhancement of 32 ppbv. For the remainder of this discussion

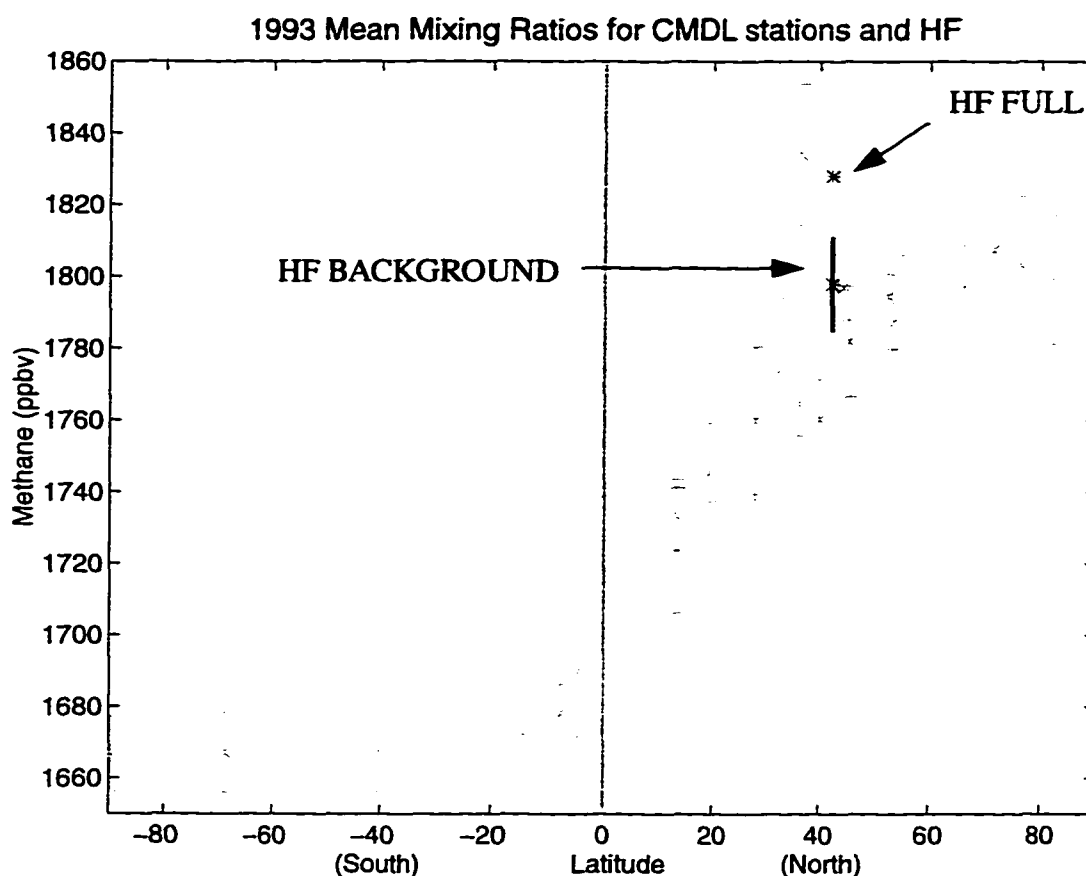


Figure 2: Concentrations of methane for the global CMDL network and Harvard Forest. X's are the mean with bar length being ± 1 standard deviation.

the terms “full” will refer to the entire database, while “background” will refer to the subset of the monthly data that uses the lower 10-30% of the data.

The background data were adjusted in order to derive the long term trend and yearly seasonal cycles. The data were detrended by subtracting a 12-month running mean from the original data, leaving cycles of 12-months or less. The data were then deseasonalized by subtracting the mean seasonal cycle of the 4-year time period from the original data, leaving the long term trend. Finally, the background data were analyzed by a least-squares algorithm to see if expected yearly and seasonal cycles existed as well as to deter-

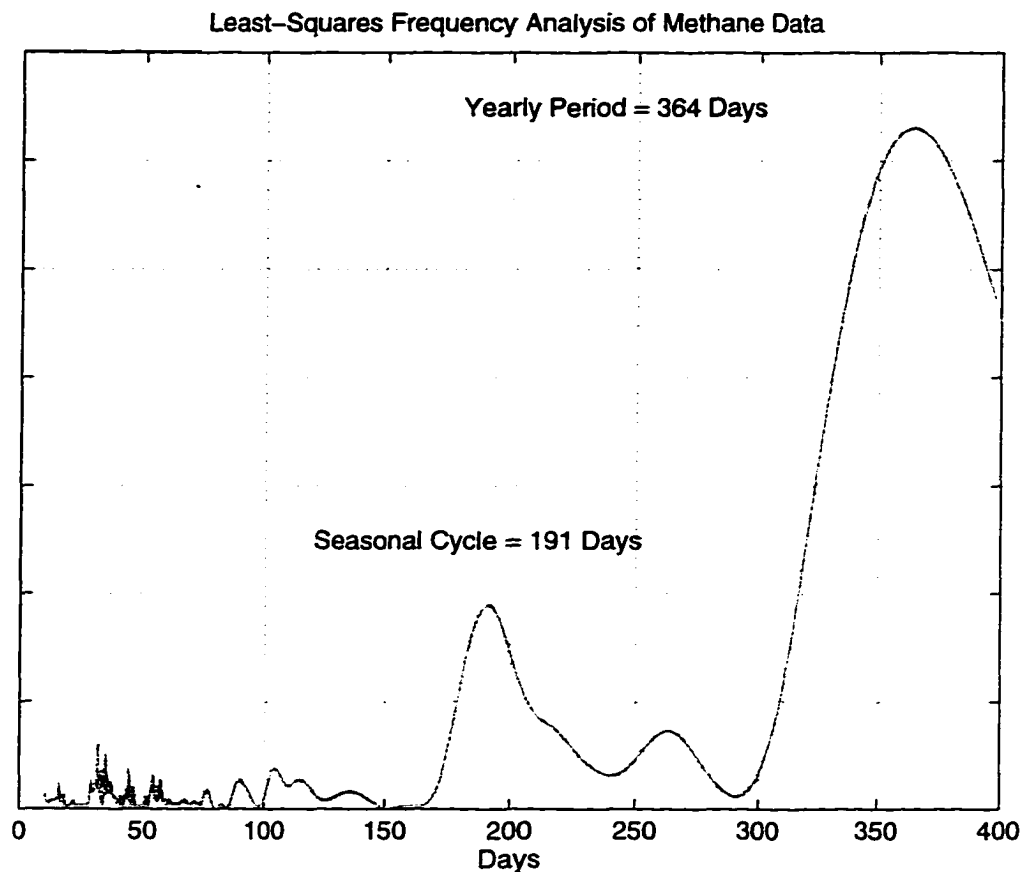


Figure 3: Least-squares frequency analysis of methane mixing ratios at Harvard Forest for 1992-1995.

mine if other unknown cycles were present [Lomb, 1976; Meeker *et al.*, 1995]. Figure 3 is the spectrum from the Lomb analysis which shows a yearly cycle of 364 days and a seasonal periodicity of 191 days. Other weak signals, especially the one centered around 260 days, appear to be the result of inter-annual variability as time of maximum and minimum CH_4 mixing ratios varies by several months from year to year.

The diurnal cycles were obtained by taking the mean of all recorded data values centered at ± 30 minutes of each hour for each day in the 4 year time period. The resulting monthly figures of the daily cycle are a composite of the four years of data and represent

highly averaged conditions.

Wind roses of selected chemical species for annual and seasonal time periods are calculated by taking the mean of all values available for the appropriate time period centered $\pm 5^\circ$ on 10° increments. For each time period the long term trend is removed and the values normalized by subtracting the average minimum value which results in a spatial distribution of enhanced concentration levels.

CHAPTER V

LONG TERM TREND, SEASONAL, AND DIURNAL CYCLES

For the 4-year time period from 1992-1995 approximately 125,000 individual CH₄ samples have been collected. Raw CH₄ mixing ratios are shown in Figure 4 while Tables 1-4 present monthly and seasonal summary statistics. The data shown in the figure and associated tables depict a variety of trends and systematic variations including: a variable upward long term trend; interannual variability; seasonal cycles; and a daily cycle which are all discussed below. In addition and perhaps most noticeable are the numerous elevated CH₄ episodes which will be discussed in a later section of this text.

5.1 Long term trend

The long term trend of CH₄ was calculated using the background data and is due to changes in global sources and sinks. The monthly median and median absolute deviation (MAD) for the full and background CH₄ mixing ratios are shown in Figure 5. From 1992 through 1995 a variable, upward trend of 5.5 ± 2 ppbv/year is observed. However, from 1992 to mid-1993 the growth of CH₄ was slightly negative, with a decrease of $-1 \pm .3$ ppbv/year for 1992. This corresponds to a time period when *Dlugokencky et al. [1994B]* also noted a sharp decrease in the growth rate of the global mixing ratios of CH₄. During the summer of 1993 the variable upward trend again resumed. On an annual basis, increases of 8 ± 2 ppbv/year, 9 ± 3 ppbv/year, and 3 ± 1 ppbv/year were observed for the years 1993, 1994, and 1995 respectively.

In the full data set, the annual median increased from 1808 to 1837 ppbv, an

Table 1: Monthly and Seasonal Summary Statistics of Methane for 1992

1992	Median (ppbv)	MAD	Mean (ppbv)	Standard Deviation	Measurement Maximum (ppbv)	Measurement Minimum (ppbv)	N (measurements)
Jan.	1830	30	1870	84	2084	1752	1186
Feb.	1827	11	1834	27	1979	1767	934
March	1823	13	1828	23	1916	1784	260
April	1813	11	1817	20	1938	1779	1001
May	1803	12	1812	32	1993	1738	4994
June	1806	23	1823	45	1978	1750	2881
July	1797	14	1804	30	1951	1743	2835
Aug.	1817	29	1838	60	2015	1755	2194
Sep.	1801	18	1816	43	1985	1729	5076
Oct.	1812	25	1834	60	2094	1743	3915
Nov.	1821	28	1838	55	2324	1761	2808
Dec.	1812	24	1845	77	2278	1760	3484
Winter	1826	46	1851	65	2084	1752	2380
Spring	1805	26	1816	36	1993	1738	8876
Summer	1802	34	1817	46	2015	1729	10105
Fall	1815	47	1839	65	2324	1743	10207
Annual	1808	38	1826	54	2324	1729	31568

increase of 29 ppbv. The annual mean increased from 1826 to 1845 ppbv, increasing 19 ppbv. Differences between the mean and median values reflect the skewed distributions in the full data set. For the background data, the median increased from 1791 to 1811 ppbv, a difference of 20 ppbv, while the mean increased from 1790 to 1811 ppbv, a difference of

Table 2: Monthly and Seasonal Summary Statistics of Methane for 1993

1993	Median (ppbv)	MAD	Mean (ppbv)	Standard Deviation	Measurement Maximum (ppbv)	Measurement Minimum (ppbv)	N (measurements)
Jan.	1823	22	1840	51	2275	1764	3121
Feb.	1817	15	1825	30	2025	1772	3531
March	1814	16	1826	34	1947	1762	3487
April	1804	12	1808	23	1908	1737	3469
May	1800	14	1805	26	1973	1741	2124
June	1796	16	1805	32	1957	1753	2407
July	1788	16	1797	31	1924	1743	2226
Aug.	1815	24	1831	50	2034	1759	1682
Sep.	1825	26	1838	50	2060	1742	2261
Oct.	1818	18	1839	53	2165	1766	3659
Nov.	1837	33	1857	62	2148	1754	2959
Dec.	1838	18	1850	41	2127	1786	2360
Winter	1818	29	1830	39	2275	1762	10139
Spring	1801	20	1806	27	1973	1737	8000
Summer	1809	36	1822	48	2060	1742	6169
Fall	1829	41	1848	54	2165	1754	8978
Annual	1815	33	1828	46	2275	1737	33286

21 ppbv. Mean annual differences between the full and background data sets for each year are about 36, 30, 40 and 34 ppbv. Any significant increase or decrease in these values over time could indicate changes in the nature of pollution events reaching the site. Within this current four year time frame, no discernible trend was evident.

Table 3: Monthly and Seasonal Summary Statistics of Methane for 1994

1994	Median (ppbv)	MAD	Mean (ppbv)	Standard Deviation	Measurement Maximum (ppbv)	Measurement Minimum (ppbv)	N (measurements)
Jan.	1838	25	1861	61	2134	1778	3887
Feb.	1840	24	1867	75	2471	1772	3206
March	1835	18	1848	38	2028	1782	3471
April	1823	18	1831	32	2007	1764	3699
May	1802	10	1812	32	1987	1763	1957
June	1811	20	1820	33	1945	1749	3041
July	1832	24	1836	39	1986	1709	2930
Aug.	1859	37	1873	59	2083	1787	842
Sep.	1811	13	1819	30	1948	1764	1426
Oct.	1850	35	1859	56	2058	1721	3097
Nov.	1843	28	1859	60	2098	1741	2799
Dec.	1860	29	1888	79	2320	1752	1736
Winter	1837	43	1858	60	2471	1772	10564
Spring	1813	26	1823	33	2007	1749	8697
Summer	1827	33	1837	45	2083	1709	5198
Fall	1850	48	1866	64	2320	1721	7632
Annual	1832	40	1847	56	2471	1709	32091

5.2 Seasonal cycles

In the northern hemisphere seasonal differences of CH₄ of 25-30 ppbv are related to changes in the oxidizing capacity of the atmosphere [Khalil *et al.*, 1993B]. On a regional scale, seasonal differences at HF are enhanced due to a complex interaction

Table 4: Monthly and Seasonal Summary Statistics of Methane for 1995

1995	Median (ppbv)	MAD	Mean (ppbv)	Standard Deviation	Measurement Maximum (ppbv)	Measurement Minimum (ppbv)	N (measurements)
Jan.	1841	22	1864	86	2467	1709	1682
Feb.	1863	22	1873	40	2097	1772	2466
March	1860	18	1873	44	2079	1783	2281
April	1845	18	1845	27	1970	1776	2184
May	1810	15	1820	32	2050	1761	2468
June	1810	18	1817	33	1941	1732	2860
July	1824	17	1830	31	2044	1755	3137
Aug.	1825	21	1833	35	1995	1761	2505
Sep.	1843	21	1852	38	2013	1793	509
Oct.	1846	20	1864	52	2142	1788	1694
Nov.	1838	19	1854	51	2072	1768	2474
Dec.	1833	17	1840	30	1985	1783	2833
Winter	1857	37	1870	57	2467	1709	6429
Spring	1820	27	1826	33	2050	1732	7512
Summer	1826	26	1833	34	2044	1755	6151
Fall	1838	31	1851	45	2142	1768	7001
Annual	1837	32	1845	46	2467	1709	27525

between local sources and sinks, as well as meteorological patterns that advect CH₄ to the site from regional urban sources. Using monthly mean background data (with trend removed) a seasonal amplitude of about 26, 24, 26, and 36 ppbv/year for the years 1992-1995 is observed (Figure 6). The seasonal cycles for the full data set have amplitudes of

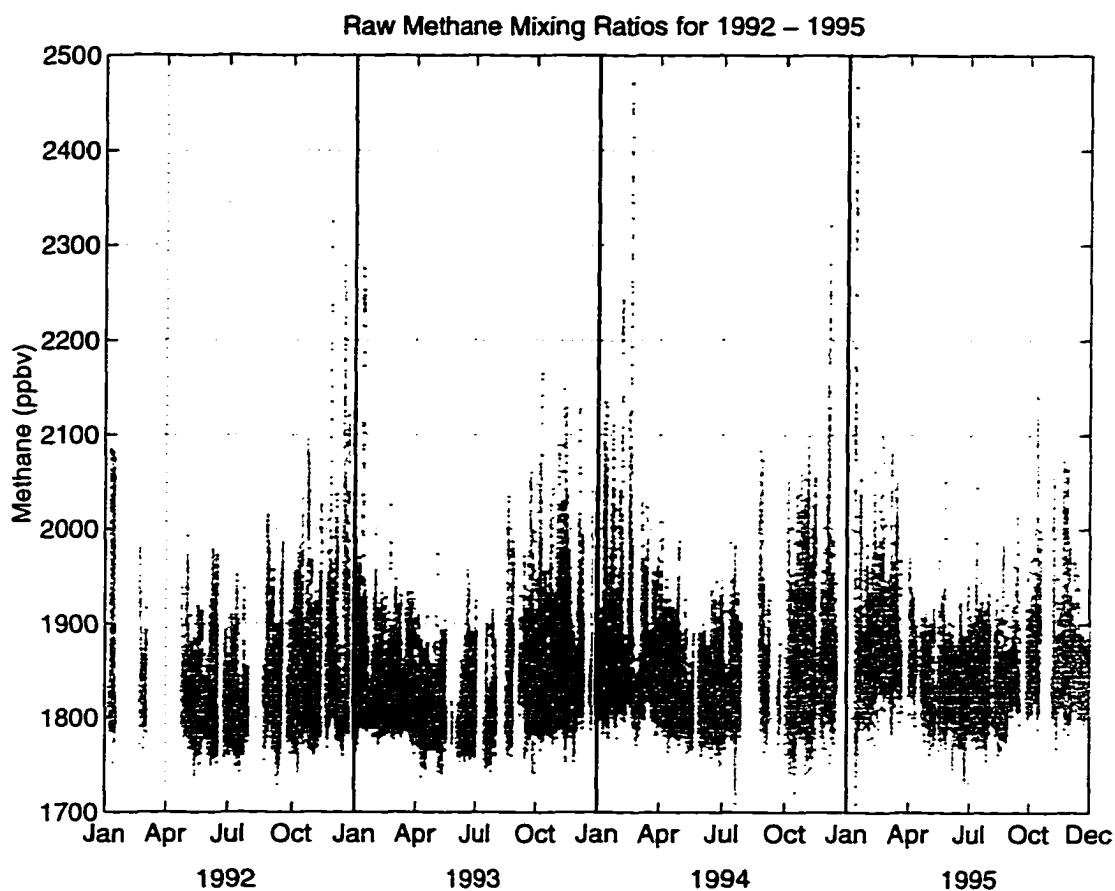


Figure 4: The atmospheric mixing ratios of methane at Harvard Forest between 1992 and 1995. These data show a variable upward trend, seasonal cycles, and the many pollution events that affect the site.

about 39, 36, 36, and 44 ppbv/year for the same time period (Figure 7). In both cases, the maximum mixing ratios occur near mid-winter and minimum ratios around mid-summer, differing by up to several months from year to year.

Subtracting the background values (as shown in Figure 6) from the full data values (as shown in Figure 7) leaves a seasonally varying residual which is shown in Figure 8. This residual between the full and background data is largest during the winter (15-21 ppbv) and smallest during the summer (11-13 ppbv) season. This pattern indicates that the effects of pollution are more pronounced in the winter than the summer. This is significant

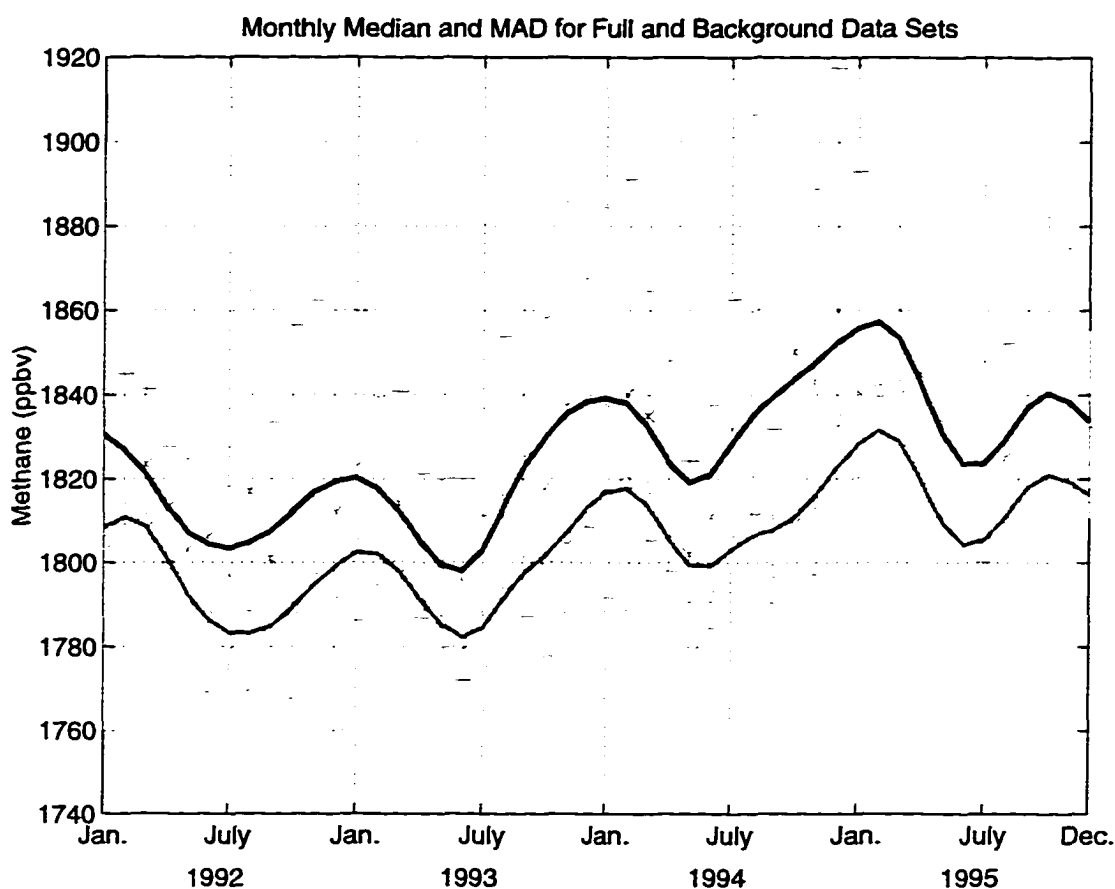


Figure 5: Monthly median and median absolute deviation of mixing ratios of methane for 1992-1995. The X's (all data) and O's (background data) represent the median mixing ratios overlaid by an error bar of ± 1 median absolute deviation. The curves are generated by robust spline fitting algorithm using the monthly data.

as the contribution by natural local sources (wetlands) is lowest in the winter, suggesting that boundary layer dynamics are the dominant controlling process over the seasons.

Changes in the seasonal differences between the full and background data over a longer time frame could be an indication of changes in CH₄ emissions.

5.3 Diurnal cycles

The mean diurnal cycle during the four year time period for each month is shown in Figures 9 A-L. Although the samples were taken during all meteorological conditions

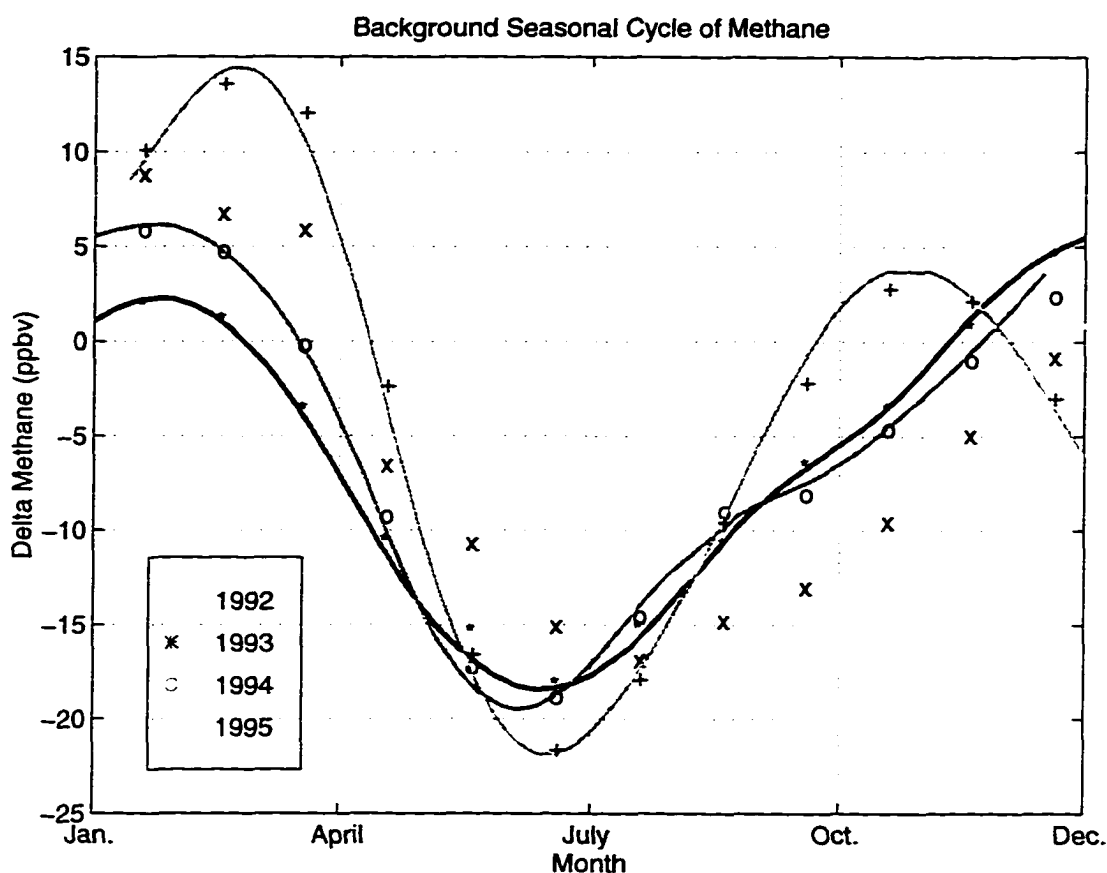


Figure 6: Background data seasonal cycles for 1992 - 1995. Symbols for each year are the monthly mean mixing ratios. Curves are generated by a robust spline fit algorithm.

and represent highly averaged CH_4 mixing ratios, the figures show cycles that change in timing and magnitude through the year. The daily maximum and minimum mixing ratios of CH_4 and differences between them (both magnitude and time) are controlled by a number of factors which vary in importance on a seasonal basis. The most important factors include changes in oxidation rates, changes in the amount of emissions from sources, the amount of solar radiation, and the extent of atmospheric stability and mixing.

From December through February (Figures 9A-C) limited vertical mixing and inputs from local sources appear to be the most important factors. Minimum values occur

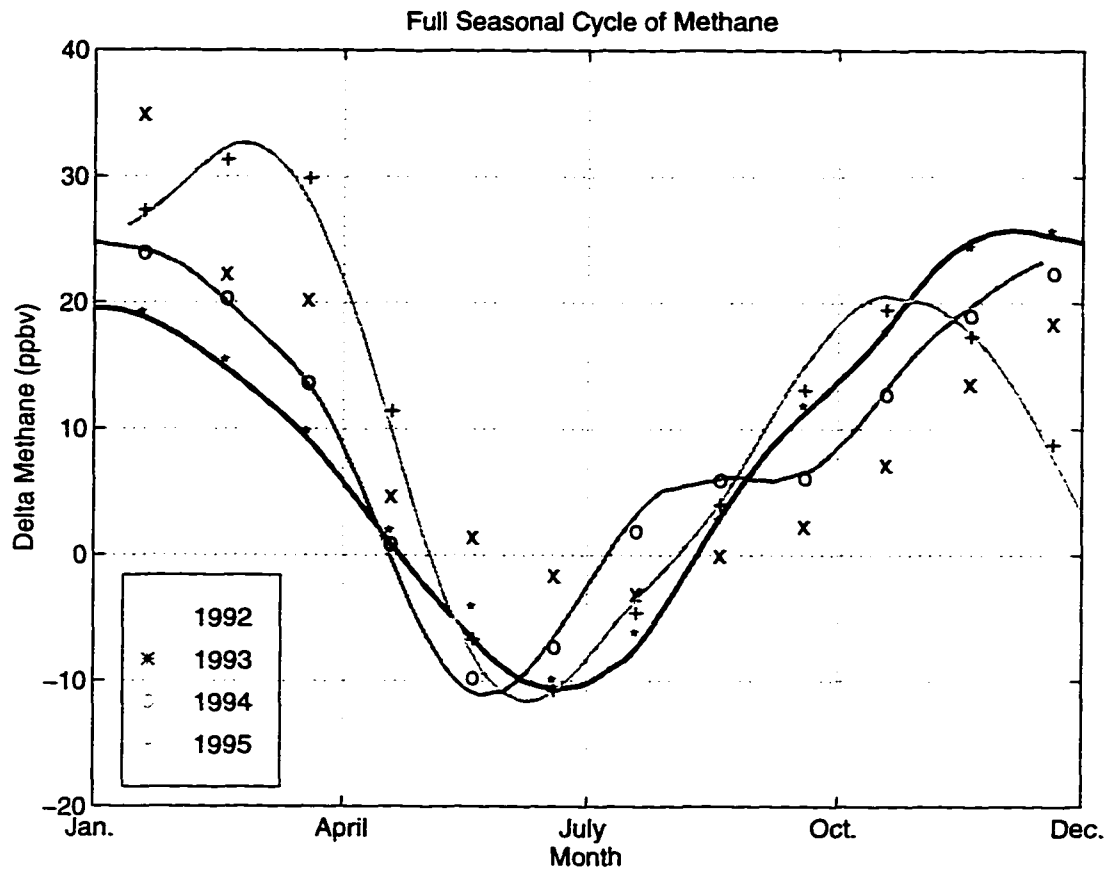


Figure 7: Full data set seasonal cycles for 1992-1995.

around 3 PM (all times local), with a gradual build up until around midnight, when values begin to decrease again. Approximately six hours elapse between the minimum concentration and the over night maximum. The average amplitude of the daily cycle for these months is about 17 ppbv. Sources of CH_4 during the winter would be primarily from local and regional landfills whose emissions continue on a year round basis [Czepiel *et al.*, 1996A, 1996B]. Although considered a small source, localized emissions from wood burning in association with home heating could also contribute to CH_4 build up during the overnight hours [Piccot *et al.*, 1996; Blaha *et al.*, in press]. With the ground frozen and generally snow covered, emissions from local wetlands are negligible during the winter

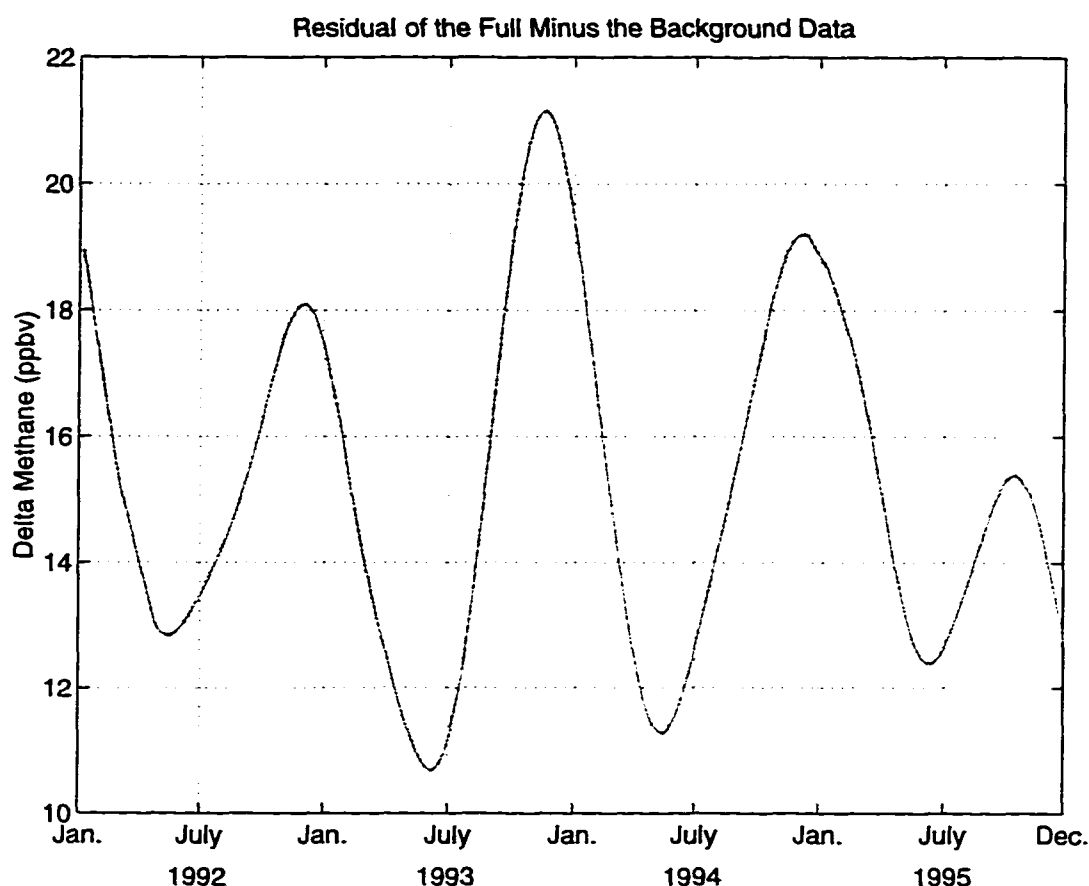


Figure 8: Residuals representing the monthly means of the full minus monthly means of the background data. The residuals are largest in the winter and smallest in the summer.

season [Melloh et al., 1996].

March and April (Figures 9 D-E) are a time of transition as solar radiation increases, temperatures begin to warm, the winter snow pack melts, and the frequency of strong night time temperature inversions decrease [Holzworth, 1967]. Inputs from nearby natural sources, mainly wetlands, however remain low and wood burning for home heating decreases. The resulting diurnal signal is very weak, with April amplitudes being the smallest during the year, around 6 ppbv.

From May through July (Figures 9 F-H) a pronounced diurnal cycle is observed.

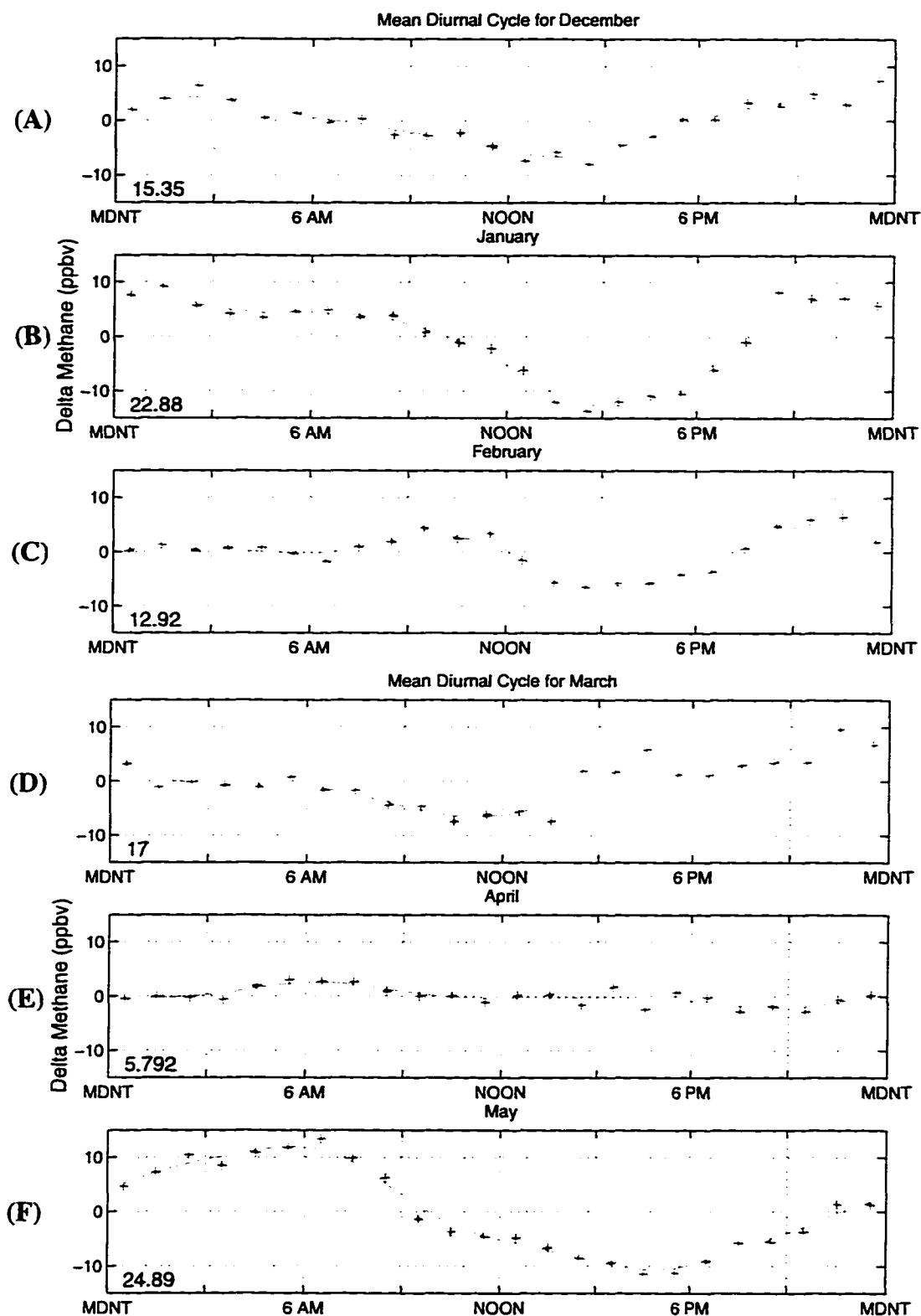


Figure 9: Mean diurnal cycle observed for each month, December-November (a-l). Number in the lower left hand corner is maximum-minimum hourly mixing ratio.

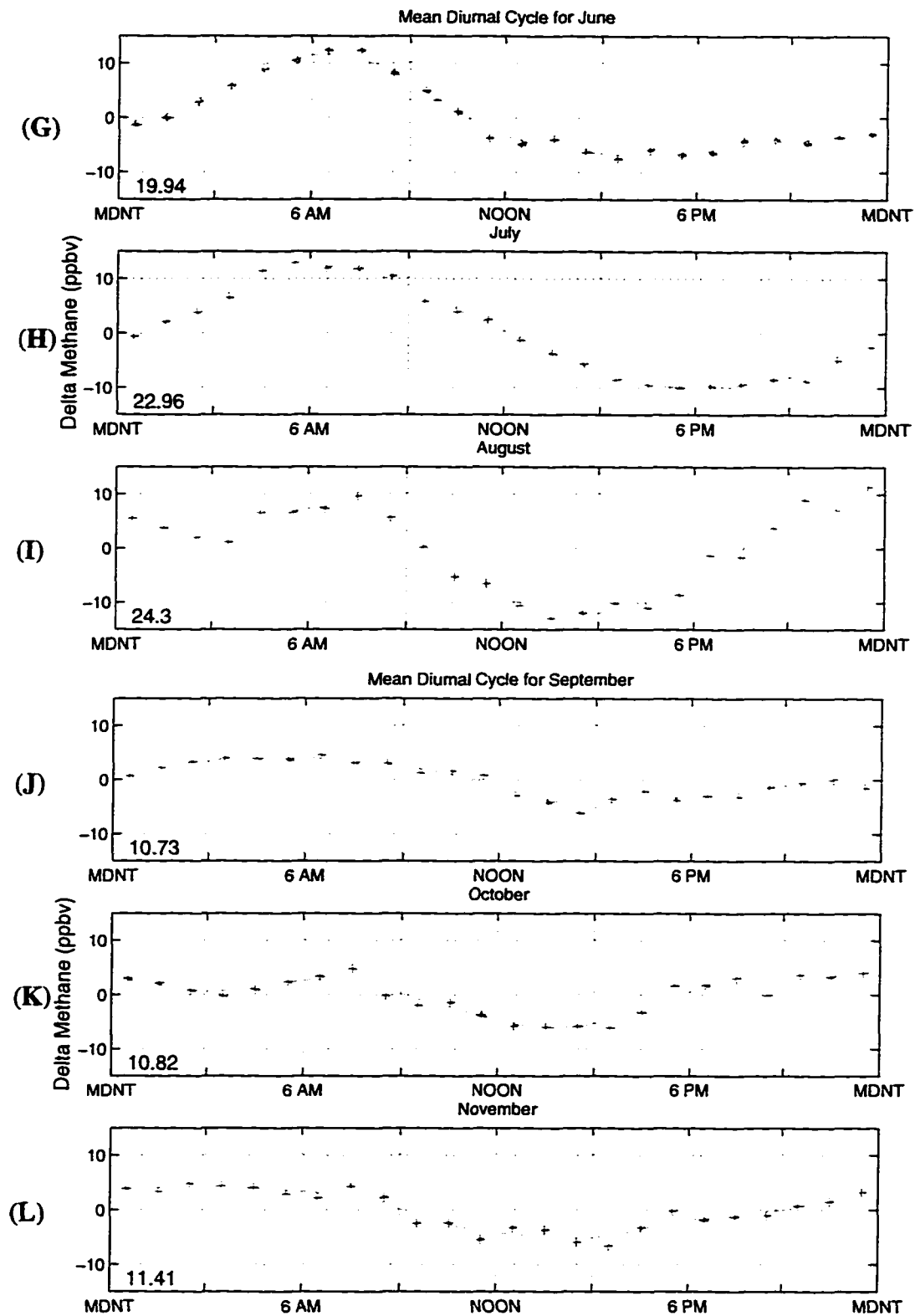


Figure 9: Mean diurnal cycle observed for each month, December-November (a-l). Number in the lower left hand corner is maximum-minimum mixing ratio.

Increasing oxidation of species by OH and emissions from nearby local sources, wetlands and landfills, become the most important factors. Minimum concentrations occur around 5 PM and begin increasing prior to sunset with the collapse of the turbulent mixed layer and continue to increase through the night reaching a maximum near sunrise at 6 AM. The period between maximum and minimum is about 12 hours, twice the winter time length. Minimum values occur during the late afternoon when the strongest vertical mixing occurs and the OH sink is large. July and August have the largest differences between maximum and minimum values of about 23 ppbv. The overnight increase in mixing ratios suggests that local sources, perhaps the nearby wetlands, are contributing to the increase.

August and September (Figures 9I-J) represent a second transitional time period when the amount of solar input is decreasing and vertical mixing is becoming less vigorous. For both months the minimum values occur around 3 PM. During August, values increase until about midnight when they begin to fall. The amplitude of the diurnal change decreases by about half (from 25 to 12 ppbv) from August to September suggesting decreasing inputs from nearby wetlands. Finally, cycles in October and November (Figures 9K-L) reflect the shorter day length and reduced local inputs from wetlands as a weak diurnal signal is observed. At this time of year the ground is still relatively warm and unfrozen, but the emissions from wetlands are decreasing and emissions from wood stoves are just beginning.

On a yearly basis the change in the diurnal cycle from month to month is for the most part gradual. However, a relatively large decrease in CH₄ is observed from March to April each year and may be due to increased oxidation by OH as longer days ensue and temperatures increase (Figure 10). By April, on average, the snow has melted and the

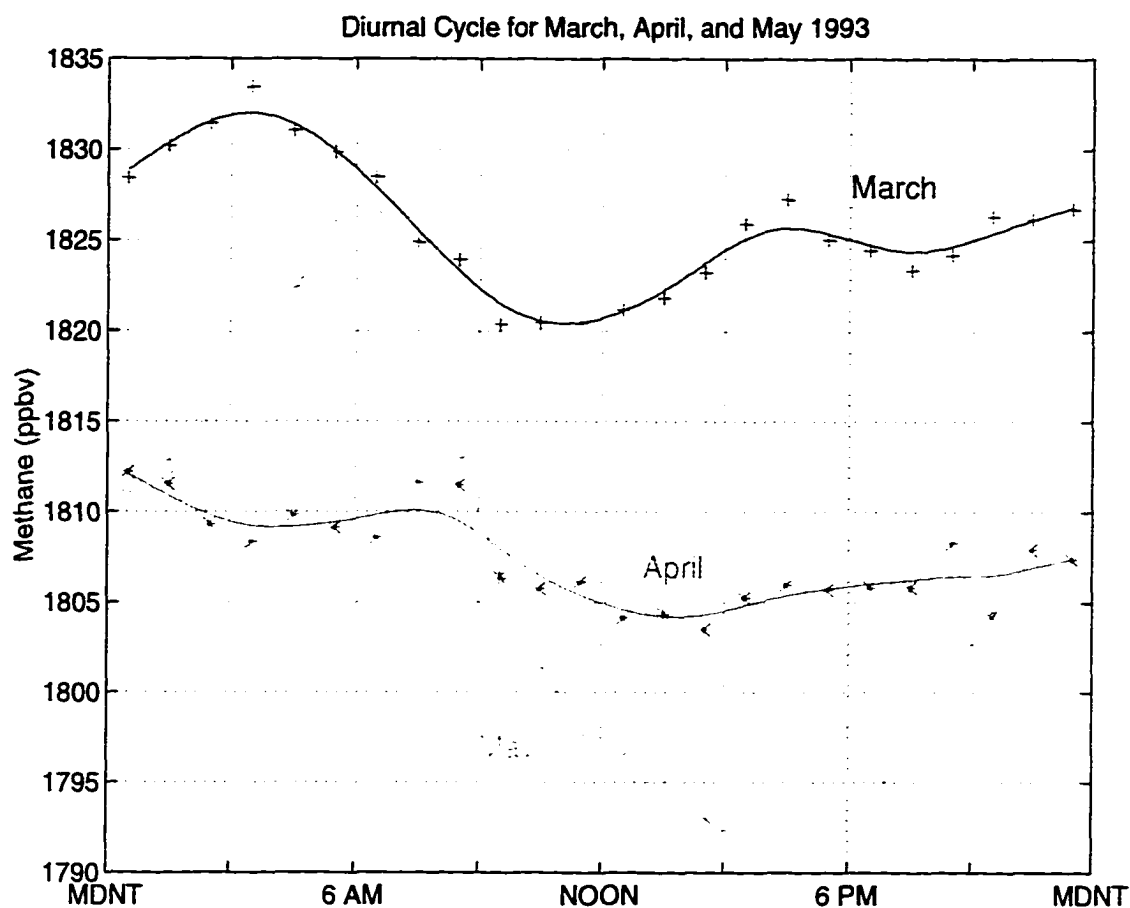


Figure 10: The mean diurnal cycle for March, April, and May, 1993.

waterlogged ground is drying allowing inputs from local wetlands to contribute to the strong diurnal cycle discussed above. Emissions from local wetlands are acting to increase the amount of CH_4 in the atmosphere at a time when removal by OH is increasing.

Opposite the spring effect, a large increase in CH_4 occurs between July and August (Figure 11) which is linked to decreasing OH oxidation. In August the diurnal cycle including over night build up continues, but by September the emissions from nearby wetlands have diminished. Similar patterns were observed for the other years.

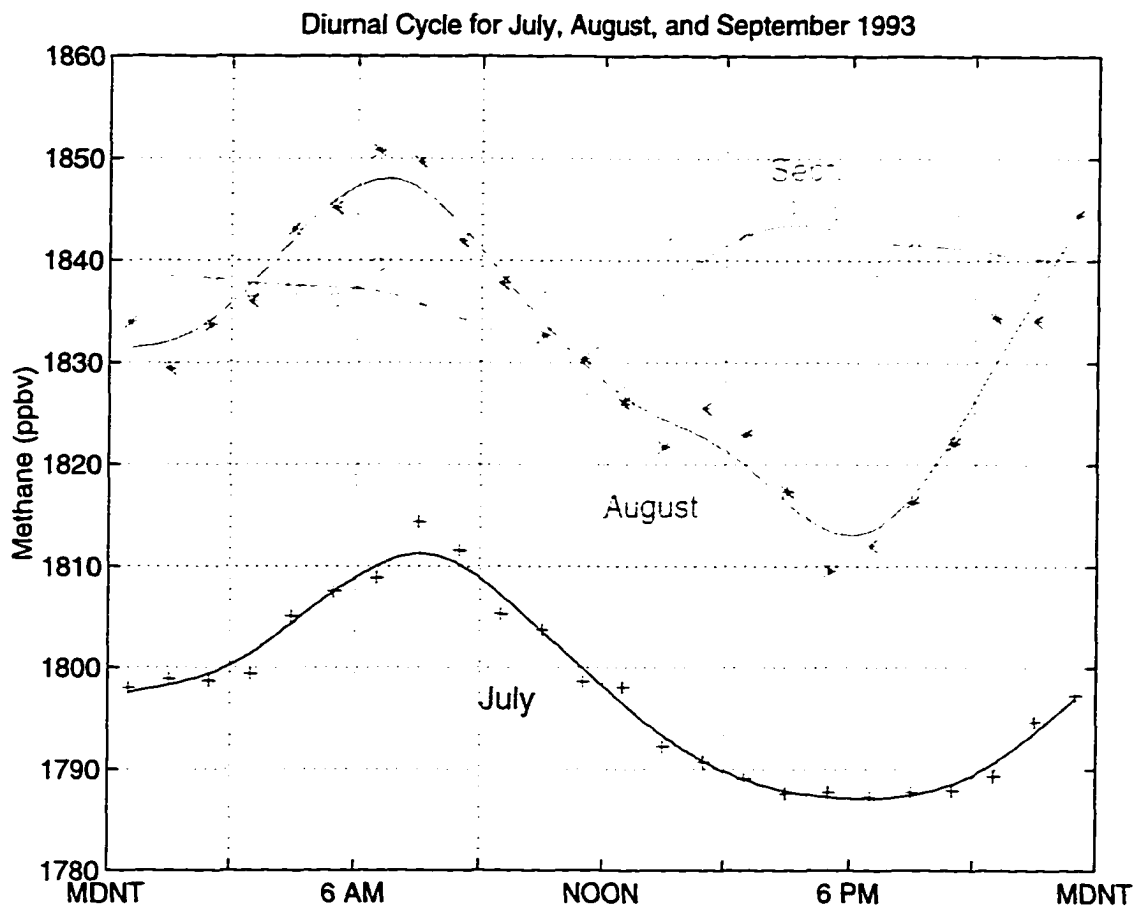


Figure 11: The mean diurnal cycle for July, August, and September, 1993.

CHAPTER VI

POLLUTION EPISODES AT THE HARVARD FOREST SITE

6.1 Location of Sources

The region surrounding the HF area is clustered with metropolitan areas. Larger cities and major highways within 250 km of the site are depicted in Figure 12, while Table

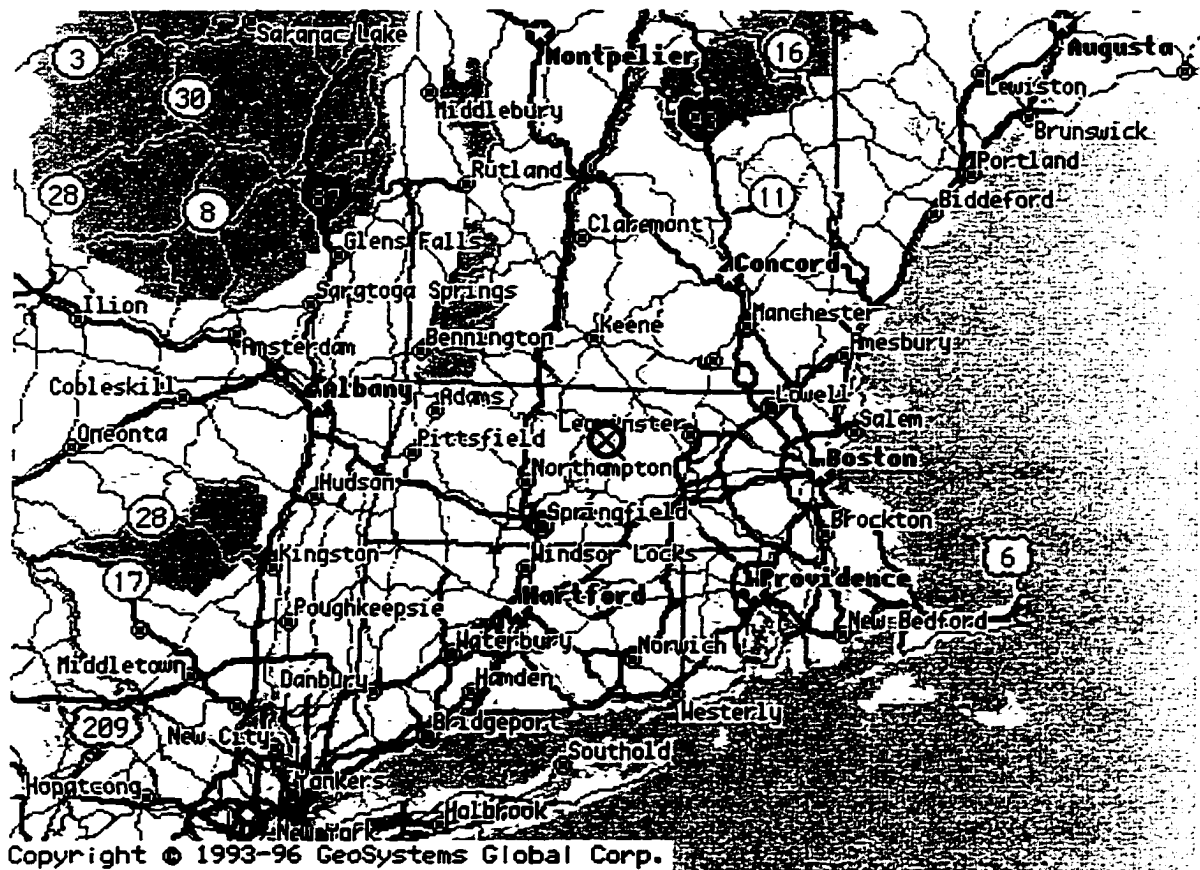


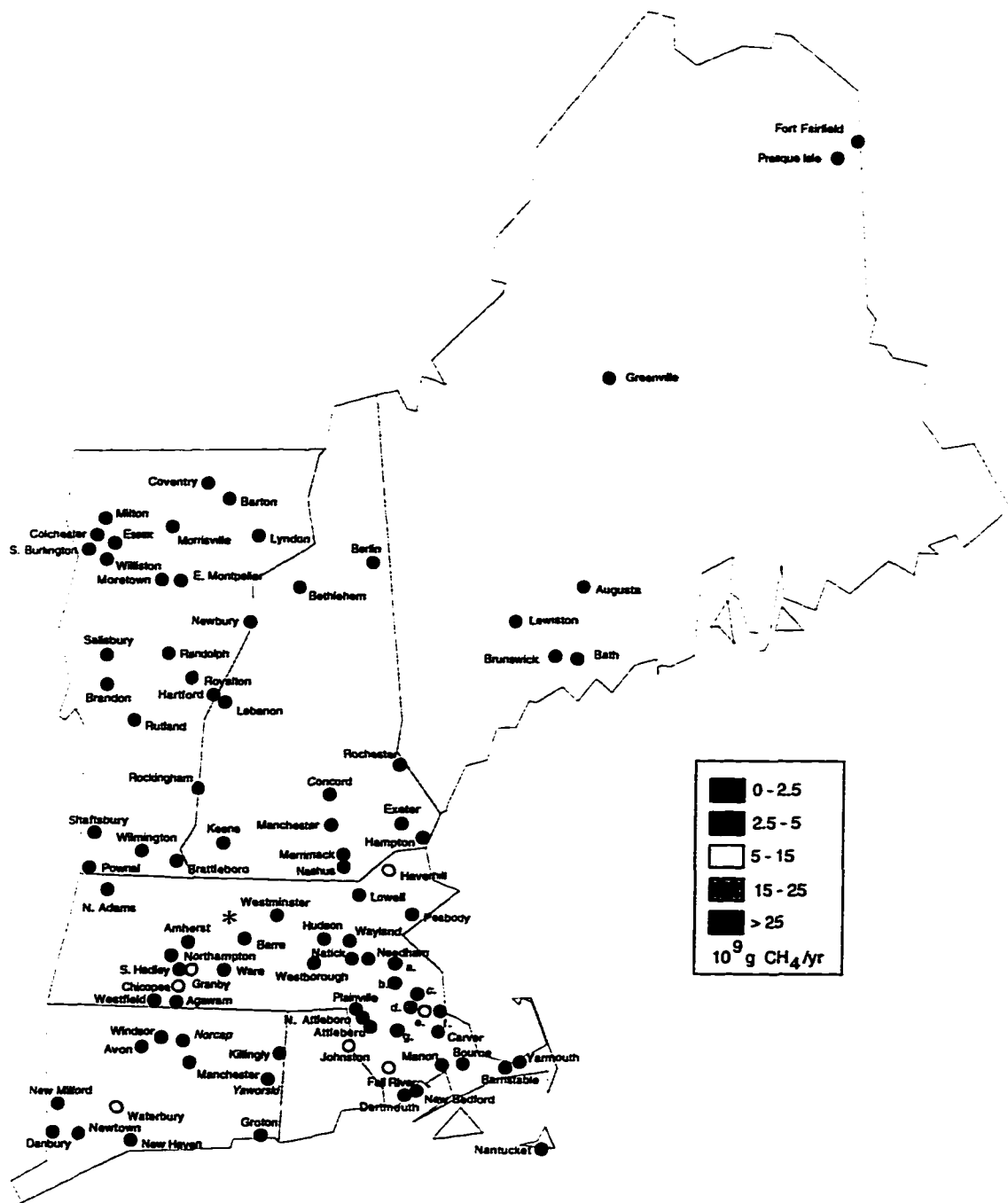
Figure 12: Regional cities and major highways surrounding Harvard Forest (X). Note the location of Springfield, MA. and New York, NY. to the southwest, Boston, MA. to the east, and Providence, RI. to the southeast.

Table 5: Heading, Distance, and Populations of Selected Cities in the Region.

City	Heading from HF to cities		Distance	Population
	degrees	direction	km	Est. 1990
Nashua, NH.	62	NE	67	80,000
Boston, MA.	99	E	94	574,000
Worcester, MA.	129	SE	41	170,000
Providence, RI.	138	SE	98	160,000
Petersham, MA.	183	S	6	1,200
Ware, MA.	190	S	26	10,000
New York, NY.	218	SW	249	7,320,000
Springfield, MA.	218	SW	54	156,000
Chicopee, MA.	223	SW	51	57,000
Granby, MA.	227	SW	37	6,000
Northampton, MA.	244	WSW	42	30,000
Amherst, MA.	245	WSW	30	35,000
Athol, MA.	329	NW	7	11,000

5 presents the heading, distance, and estimated 1990 population for selected localities. The location and estimated source strengths of known active landfills surrounding HF is shown in Figure 13, with Table 6 listing their heading and distance from the site.

The largest sources of CH₄ in the Northeastern U.S. are wetlands and landfills which contribute 46% and 39% of the regions total respectively [Blaha *et al.*, *in press*; EPA, 1993]. However, these two dominant sources are in distinctly different locations. In Maine 89% of emissions are estimated to come from wetlands, primarily in the late spring and summer. In Massachusetts, where HF is located, 82% of emissions are estimated to be



a. Milton b. Randolph c. Rockland d. East Bridgewater e. Halifax f. Plymouth g. Taunton

Figure 13: Landfills surrounding Harvard Forest (*). The strongest sources closest to HF are located at Peabody, MA. to the east and East Bridgewater and Plainville, MA. to the southeast. Note the nearby cluster of landfills to the southwest of the site. (Figure courtesy *Blaha et al., in press.*)

Table 6: Heading and Distance to Regional Landfills.

Landfill Name	Heading from HF to landfill		Distance	Transport Time at 2m/s
	degrees	direction	km	hours
Merrimack, NH.	53	NE	71	10
Nashua, NH.	62	NE	67	9
Westminster, MA.	74	ENE	24	3
Peabody, MA.	87	E	104	15
E. Bridgewater, MA.	116	SE	113	17
Plainville, MA.	127	SE	89	12
Barre, NH.	137	SE	10	1
Johnston, RI.	138	SE	98	14
Southbridge, MA.	165	SSE	48	7
Ware, MA.	190	S	26	4
Chicopee, MA.	223	SW	51	7
Granby, MA.	227	SW	37	5
Northampton, MA.	244	WSW	42	6
Amherst, MA.	245	WSW	30	4

from landfills on a year round basis. As a consequence of the climate action plan, a nationwide strategy to regionalize landfills which have CH₄ gas collection systems is well underway. In the New England region the number of operating landfills has decreased from 507 in 1990 to 151 in 1995, with six of them having CH₄ recovery systems [*Blaha et al., in press; Bogner et al., 1995*]. While a small component of the total U.S. emissions, wood burning may be a significant source of CH₄ and other combustion by-products in rural areas such as HF during the winter heating season. Other sources such as cars and trucks,

ruminants, and natural gas leakage are believed to be a very minor part of the total measured CH_4 emissions in the HF region [Piccot et al., 1996; Blaha et al., in press].

6.2 Characterizing the Harvard Forest flow regime

In addition to CH_4 , other chemical species including acetylene (C_2H_2), propane (C_3H_8), ethane (C_2H_6), hexane (C_6H_{14}), and 1,3-butadiene (C_4H_6) are plotted as a function of wind direction on annual and seasonal time periods in order to discriminate between man made and natural sources and to quantify the varying effects of local, regional, and distant transport to the site. A clean air quadrant to the northeast is also examined and compared to the other anthropogenically influenced sectors. Detailed case studies are used to identify possible sources and identify the atmospheric conditions and transport pathways which lead to the most severe pollution events.

Based on the observed enhancements found in the wind roses, specific quadrants influenced by pollutants are examined in more detail through the use of additional species with differing sources and lifetimes. Approximately 20 species are measured at HF and table 7 gives a partial listing of them along with their primary sources and estimated summer and winter lifetimes. C_2H_2 is solely from combustion and is used as a tracer for an anthropogenic signature. A strong correlation between CH_4 and C_2H_2 would indicate that anthropogenic sources are the dominant component of the total measured signal. A strong correlation between CH_4 and short lived species such as C_6H_{14} , 1,3-butadiene, or t-2-pentane (C_5H_{10}), implies transport from nearby sources in which the short lived species have had insufficient time to be oxidized. The ratio of C_3H_8 and C_2H_6 is used to discriminate between wood burning or liquefied natural gas (LNG). Lower ratios of 0.3-0.5 are associated with wood burning, while ratios approaching 1 are associated with LNG [D. R. Blake

Table 7: Primary Sources and Estimated Lifetimes* for Selected NMHC's

Species		Primary Source	Summer Lifetime	Winter Lifetime
			Days	Days
Acetylene	C ₂ H ₂	Combustion	7	116
Ethane	C ₂ H ₄	Natural Gas	38	450
Propane	C ₃ H ₆	Natural Gas/ Petrochemical Industries	8	87
Butane	C ₄ H ₁₀	Auto Exhaust	3.4	36
Pentane	C ₅ H ₁₂	Auto Exhaust	2.2	23
Hexane	C ₆ H ₁₄	Combustion	1.5	15
1,3-Butadiene	C ₂ H ₆	Combustion	0.125	2
t-2-pentene	C ₅ H ₁₀	Combustion	0.125	2

*Lifetimes are based on a rate constant as used by Goldstein et al., 1995

et al., 1996; N. J. Blake et al., 1996].

Detailed case studies are used to examine the most severe pollution events and utilize daily streamline maps at various pressure levels and backward air mass trajectories to examine probable transport pathways. The isentropic trajectory package was originally received from the National Center for Atmospheric Research and has been modified extensively since [Danielson, 1961; Haagenson et al., 1979; Shipham et al., 1994]. Products from the National Climate Data Center were used to determine regional snow depth, percent of possible sunlight, maximum and minimum temperature, and precipitation type and amount.

6.3 Wind Direction and Speed

Wind frequencies for the four year time period, the four winter seasons (January-March), and the four summer seasons (July-September), are shown in Figures 14 a-c. The prevalent wind direction during the winter is from the northwest (NW), which generally transports cleaner air from Canada. The prevalent summer wind is from the southwest (SW), which transports air across many potential anthropogenic sources and can be associated with periods of stagnation and corresponding pollution events. While a westerly component dominates the mean flow, transport from other quadrants does occur and maritime air on occasion reaches the site whenever there is a persistent wind flow from a southerly or easterly direction.

As with wind direction, wind speed varies seasonally as shown in Figures 3 d-f. On an annual basis, the fastest winds (2.5-3 m/s) are from the west and north and also from a small area to the east. The lightest winds (2 m/s) are from the NE and the south. Winter winds are stronger than the annual average and are strongest (3-3.5 m/s) from the west and NW and also to the east. The lightest winter winds (2 m/s) are from the southeast (SE) to the SW. Summer winds are greatest (2.5 m/s) from the NW to north and to the east, while the lightest winds (1.5 m/s) are from the south and SW and the NE.

Knowledge of the wind flow patterns combined with locations of potential sources provides an indication of which quadrants will likely be effected by anthropogenic by-products. Large cities are located to the east, south, and west of the site, while the three largest landfills are located to the east and SE. Anthropogenic influences should be the strongest in the quadrants where these sources are located. Conversely, the lowest populations and fewer landfills are to the north and NE of the site in which cleaner air should be

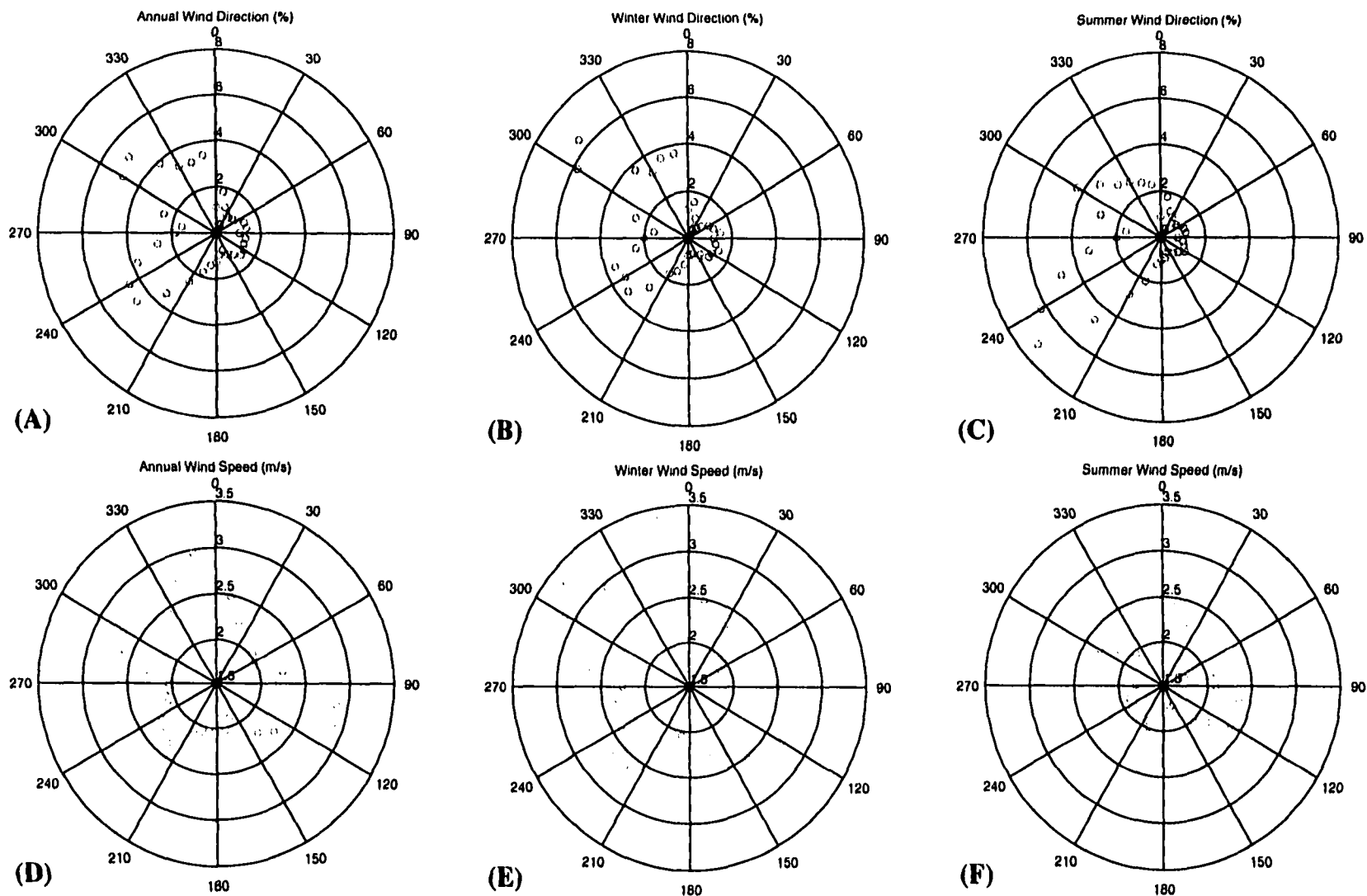


Figure 14: Wind direction (%), (a-c) and speed (m/s) (d-f) at the Harvard Forest tower for annual, winter, and summer time periods.

expected.

Particular wind flow patterns can be linked to recurring synoptic conditions [*Brook et al., 1994, 1995; Holzworth, 1967*]. The prevalent SW summer flow is often associated with the circulation around the “Bermuda” high which is associated with warm and humid conditions and very light winds. Stronger winds associated with Nor’easters moving up the East coast are seen when the flow is from the east and SE and are associated with stormy conditions. A NW flow is often associated with cold unstable air moving in from Canada and signals fair weather conditions. Understanding the character of these major wind flow regimes provides additional insight about atmospheric conditions, which in turn can be related to the complex chemical signal observed at the site. Additional factors besides prevailing seasonal winds make any simple link between the location of sources and corresponding enhancements in chemical species difficult. They include terrain effects that may channel pollutants, seasonal variations in source emissions, and yearly variability in wind patterns.

6.4 Methane Enhancements

CH₄ enhancements for the annual, winter, summer, and winter minus summer time periods are shown in Figures 15 a-d. For the four year period, enhancements of about 60 ppbv are observed in the heavily industrialized SW high emissions sector (HES) centered on 250°. The smallest enhancements (0-10 ppbv) are in a clean air sector (CAS) to the NE centered on 40°. Other enhancements are to the east and south of the site and exceed 30 ppbv at 90°, 120°, 150° and 170°.

Winter enhancements are larger than those observed in the summer due to a combination of the reduced oxidation of species and more frequent pollution events. During

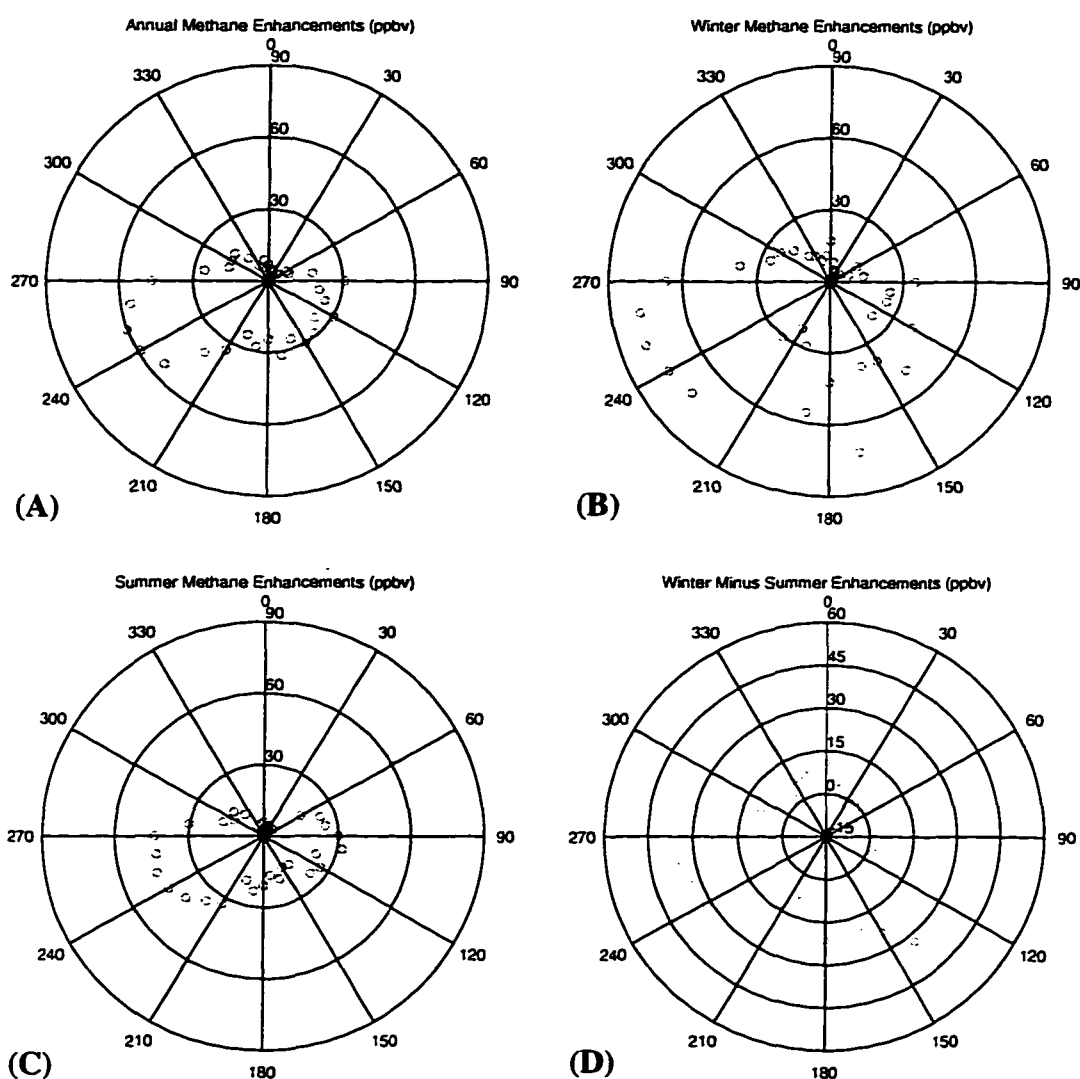


Figure 15: Enhanced methane mixing ratios for (a) annual, (b) winter, (c) summer and, (d) winter-summer time periods.

the winter seasons, the HES enhancement is 75 ppbv as compared to 45 ppbv during the summers. Variable enhancements occur east and south of the tower, with values exceeding 30 ppbv at 90°, 120°, 140 to 200°, including a large enhancement of 73 ppbv at 170°. In the summers, enhancements to the east and south exceed 30 ppbv only at 90 and 100°, and the large winter time enhancement at 170° is not observed.

Seasonal enhancement differences are largest in the more polluted sectors and

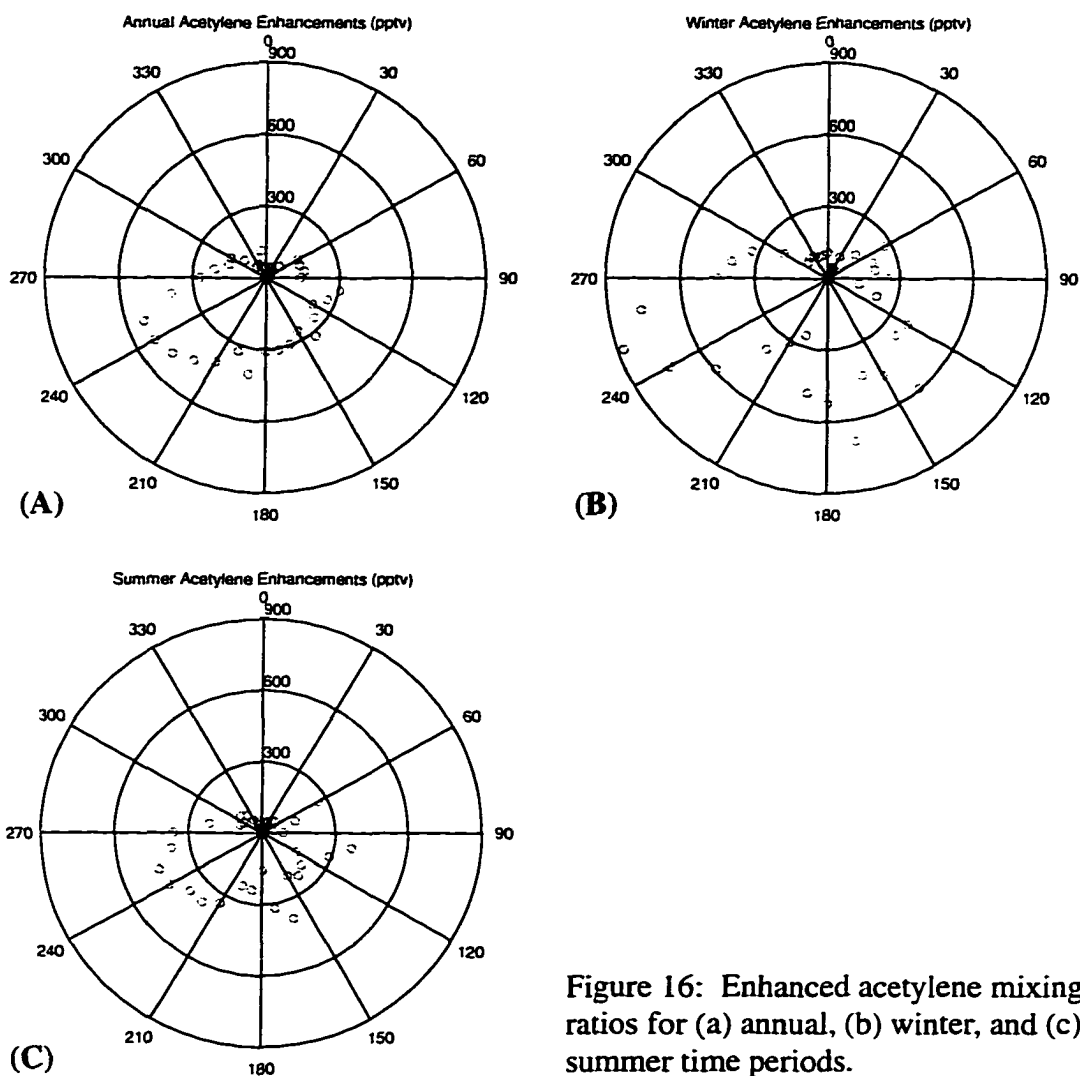


Figure 16: Enhanced acetylene mixing ratios for (a) annual, (b) winter, and (c) summer time periods.

smallest in the CAS. In the HES, the 35 ppbv difference is similar to the seasonal cycle that was found for the full HF data set which includes pollution events. The greater differences between seasons at 140°, 190°, and especially 170° appear to be due to winter time pollution.

6.5 Acetylene Enhancements

C_2H_2 is solely derived from combustion and enhancements of it are compared to those that are observed for CH_4 in Figures 16 a-c. On an annual basis the largest C_2H_2

enhancements of about 500 pptv occur in the HES. Other enhancements are found to the south and east with values exceeding 300 pptv at 100 and 140°. Enhancements are again lowest in the CAS. In the winters, the HES enhancements reach a maximum of 900 pptv. A second area of values greater than 300 pptv is observed SE of the site, with enhancements exceeding 600 pptv at 140° and 170°. In the summers, enhancements of 450 pptv, about half the winter value, are observed in the HES. Other enhancements exist NE to east to south of the site, with values exceeding 300 pptv at 100°, and 160-170°.

The similarities in enhancement patterns between CH_4 and C_2H_2 reinforces the hypothesis that CH_4 mixing ratios are linked to anthropogenic sources due to the co-location of landfills and cities. This appears to be the case in the HES where numerous cities and landfills are co-located about 40-50 km from the site. In some wind sectors, differences in the relative enhancements of CH_4 and C_2H_2 are due in part to differing locations of strong sources. For instance, the relative enhancement of C_2H_2 at 60° in the summer and winter is stronger than is observed for CH_4 . In this case the combustion source may be the city of Nashua, NH., 62 km distant, which has only small known landfills in its vicinity.

6.6 Summer Hexane and 1,3-Butadiene Enhancements

The short summer life time of C_6H_{14} (~1.5 days) and C_4H_6 (~ 3 hours) can be used as a proxy to infer the age of chemical species measured at HF (Figures 17 a-b). These life times assume sunny conditions and must be adjusted upward to account for night time periods and the percent of possible sunshine, which increases the estimated lifetime to 2 - 3 days for C_6H_{14} and 3-8 hours for C_4H_6 .

C_6H_{14} enhancement patterns are similar to those that are observed in CH_4 . The

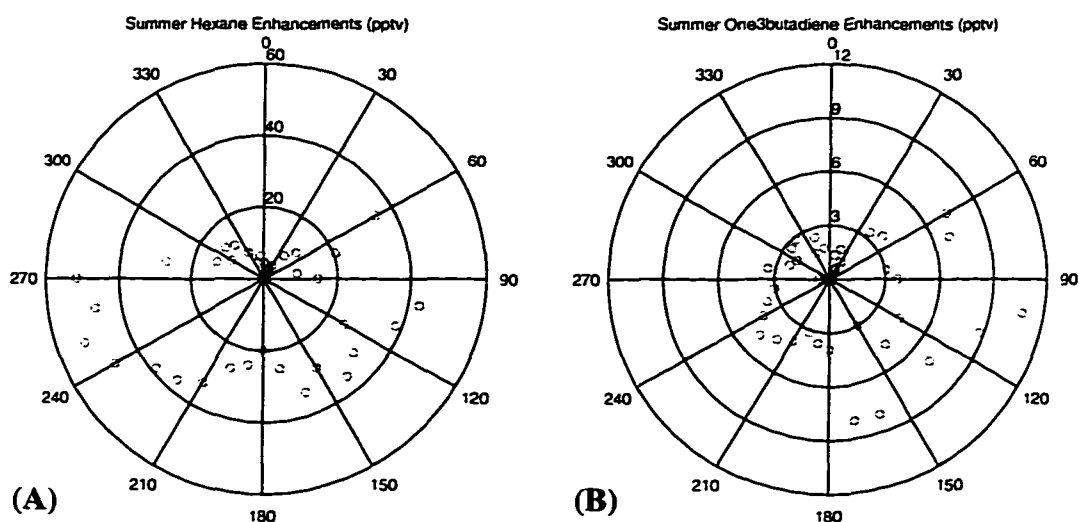


Figure 17: Summer enhanced (a) hexane and (b) 1,3-butadiene mixing ratios.

largest enhancements (~ 50 pptv) occur in the HES. Large enhancements in the $100\text{--}110^\circ$ wind quadrant reflect a combination of a fast mean wind speed (see Figure 3F) and generally cloudy conditions which limits mixing and oxidation of species. Other enhancements exceeding 30 pptv are seen at 60° and $130\text{--}140^\circ$. Lower enhancements, such as are found in the CAS, reflect a chemically aged air mass that has not been in contact with anthropogenic sources for at least several days.

Enhancements in C_4H_6 are largest to the SE instead of the SW HES as has been found for other longer lived species. The lower values in the HES implies pollutants in that sector may be older than those in the SE quadrant. However, this could be a function of stagnant conditions and light winds that are common in the summer SW flow. The shift in enhancements implies that the age of the species in the HES is somewhere between 8 hours and 2.5 days old. Large enhancements at $170\text{--}180^\circ$ must be of local origin and appear to be from the near by town of Petersham. Enhancements at $100\text{--}110^\circ$ may be

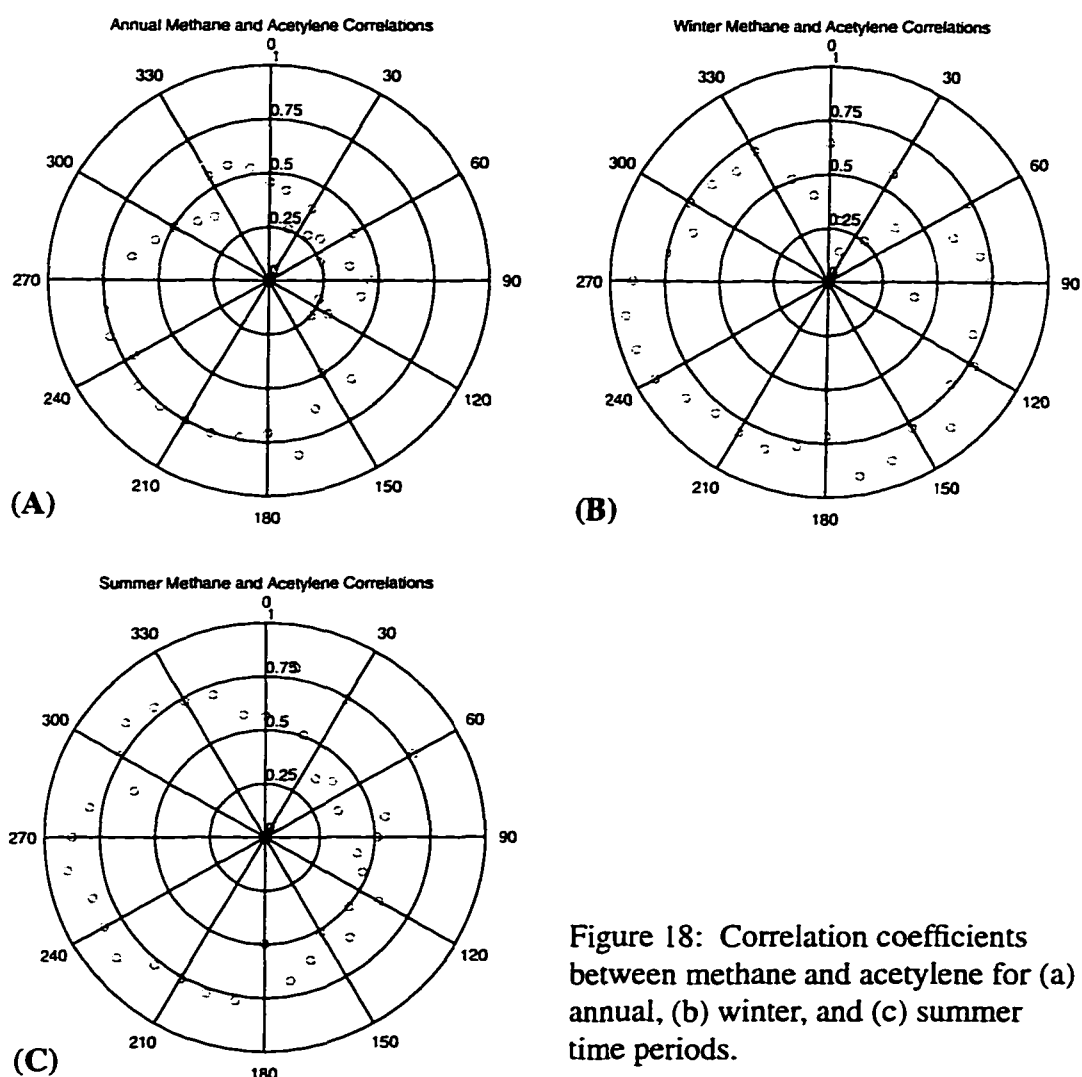


Figure 18: Correlation coefficients between methane and acetylene for (a) annual, (b) winter, and (c) summer time periods.

linked to the small town of Barre, 10 km distant, while enhancements at 60° are likely from Nashua, NH. The change in enhancement patterns between these two short lived species shows the utility of using them as a proxy to infer the age of pollution. The use of other short lived species with intermediate life times could further help define the age of the sources.

6.7 Correlations between Methane and Acetylene

Correlation coefficients for CH_4 and C_2H_2 as a function of wind direction for the annual and seasonal time periods are shown in Figures 18 a-c. The annual correlations are

high and fairly uniform to the south and west with values generally exceeding 0.75. The strong correlations, especially in the HES, reflect fresh emissions that have not had time to be mixed or diluted. This is an indication that the anthropogenic signal HF receives from these populated areas persists on a year round basis. Correlations are lower and more variable (.25-.70) east and south which may be due to better mixing and incursions of maritime air. In the CAS, the low correlations (.25-.40) are due to a well mixed, aged air mass with out any significant anthropogenic inputs.

Seasonal correlations between CH_4 and C_2H_2 remain high especially in the winter when transport to the site is faster and atmospheric mixing is reduced. During the winter seasons correlations exceed .75 from the SE to the south and to the west reaching a maximum of .95 in the HES. Correlations in the CAS are lower and quite variable ranging from .10 to .60. During the summers correlations remain high in a large area from east to south to west to north of the site. In the HES, correlations are again around .95. Such tight correlations in light of slower summer winds and increased mixing implies nearby sources. Low correlations in the CAS imply an aged air mass in which mixing ratios of C_2H_2 have been depleted.

6.8 Summer Correlations between Methane and Short Lived Species

Summer correlations between CH_4 and two short lived species, C_6H_{14} and C_4C_6 , can be used to infer the age of chemical species reaching the site (Figures 19 a-b). Correlations between CH_4 and C_6H_{14} are around .75 in the HES, similar to what is observed between CH_4 and other longer lived species. The age of the species measured is less than the age of C_6H_4 since its high correlations with CH_4 implies there has not been time for much mixing. Correlations range from .5 to .75 in other sectors, excluding the CAS where

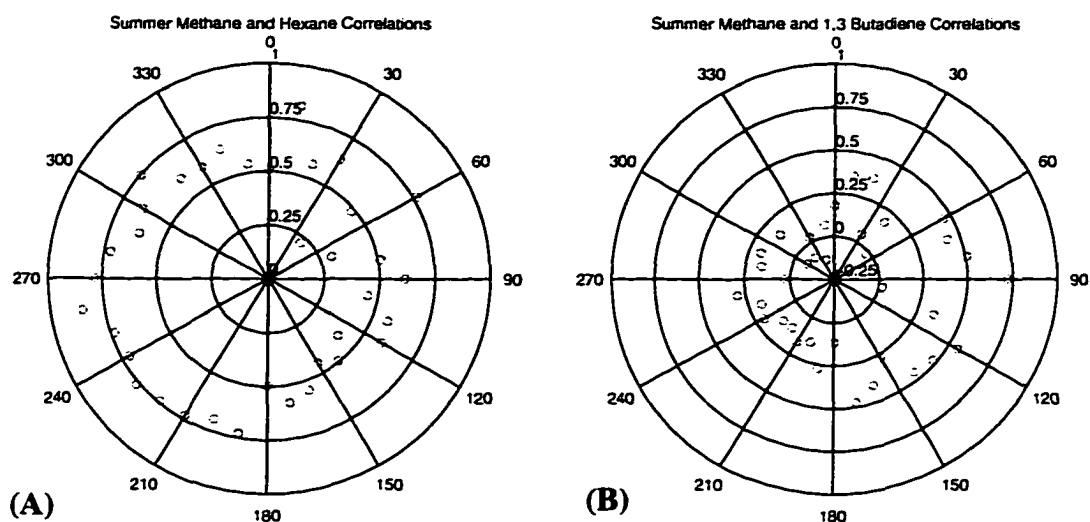


Figure 19: Summer correlations between (a) methane and hexane and (b) methane and 1,3-butadiene.

they are less than 0.5.

Correlations between CH_4 and C_4C_6 are much lower than was found between CH_4 and C_6H_{14} and have a different pattern. The lower correlations in the HES infer that C_2H_6 is being oxidized prior to the time it would take for it to reach the tower. Using mean summer winds of 1.5 m/s in this quadrant converts to a mean transport time of about 8 hours. This is greater than the 6 hours estimated life time of the species and is consistent with its partial depletion. Higher correlations to the SE may be due to faster wind speeds and more cloud cover as compared to the SW sector. Correlations around zero in the CAS indicate C_2H_6 has been depleted in this sector prior to reaching the site which is consistent with an aged air mass.

CHAPTER VII

THE CHEMICAL SIGNATURE OF THE HF REGION

The chemical composition of four quadrants most impacted by anthropogenic pollutants is examined in detail to quantify how CH_4 and other combustion sources at varying distances and strengths impact the site. The HES includes the combined emissions from Springfield, Northampton, and Amherst, MA. The city of Boston impacts the 90-100° wind quadrant, Providence, RI. and Worcester, MA. (PW) the 120-140° wind quadrant, and the nearby town of Petersham the 170° wind sector. In contrast to the polluted quadrants, the composition of the CAS is also examined. Table 8 presents summary statistics for selected chemical species in each sector.

7.1 The High Emissions Sector

The HES enhancements are the largest observed and are a result of the combined outflow of cities clustered in that sector. CH_4 is plotted against C_2H_2 , C_6H_{14} , C_3H_8 , and C_2H_4 in Figures 20a-d. Mean winter minus summer mixing ratio differences are 55 ppbv for CH_4 , 1.04 ppbv for C_2H_2 , 0.04 ppbv for C_6H_{14} , 1.42 ppbv for C_3H_8 , and 2.21 ppbv for C_2H_4 . These seasonal differences are larger than would be expected due to oxidation of species alone [Khalil et al., 1993B]. Extreme mixing ratios of all species are observed in both seasons with a maximum mixing ratio of 2471 ppbv of CH_4 during the winter. Such high mixing ratios represent fresh emissions and must be from a nearby source. Correlations between CH_4 and the other plotted species are consistently high in both seasons, exceeding 0.90 in the winter and 0.75 in the summer and implies that a well mixed local

Table 8: Mean and Standard Deviation for Selected Wind Quadrants

SPECIES	HES		CAS		Providence, RI/ Worcester, MA.		Boston, MA.		Petersham, MA.	
	(250°)		(40°)		(120-140°)		(90-100°)		(170°)	
	Winter	Summer	Winter	Summer	Winter	Summer	Winter	Summer	Winter	Summer
	Mean (SD)	Mean (SD)	Mean (SD)	Mean (SD)	Mean (SD)	Mean (SD)	Mean (SD)	Mean (SD)	Mean (SD)	Mean (SD)
CH ₄ (ppbv)	1899 (89)	1844 (44)	1824 (22)	1803 (22)	1858 (54)	1821 (34)	1846 (31)	1837 (26)	1884 (71)	1824 (36)
C ₂ H ₂ (ppbv)	1.69 (1.04)	.65 (.37)	1.02 (.25)	.26 (.12)	1.41 (.51)	.47 (.24)	1.01 (.29)	.58 (.42)	1.56 (.79)	.43 (.21)
C ₆ H ₁₄ (ppbv)	.10 (.09)	.06 (.04)	.04 (.01)	.02 (.01)	.09 (.06)	.05 (.04)	.06 (.02)	.05 (.04)	.13 (.12)	.04 (.03)
C ₃ H ₈ (ppbv)	2.29 (1.09)	.87 (.41)	1.55 (.31)	.43 (.21)	1.81 (.49)	.63 (.27)	1.47 (.37)	.87 (.45)	2.00 (.85)	.64 (.24)
C ₂ H ₄ (ppbv)	3.98 (1.46)	1.77 (.55)	2.84 (.43)	1.29 (.25)	3.18 (.61)	1.47 (.38)	2.63 (.41)	1.70 (.61)	3.63 (1.25)	1.49 (.34)

source of pollutants is observed on a year round basis. Terrain affects of the near North to South alignment of the valley that these cities are located in coupled the prevailing SW flow may channel pollutants to the HF location and enhance the possibility for severe pollution events to occur.

7.2 The Clean Air Sector

The chemical composition of the CAS (Figures 21 a-d) is dominated by chemically aged air masses that have not had contact with anthropogenic sources for at least several days, likely considerably longer. Mean winter minus summer differences are 21 ppbv for CH₄ (as compared to 55 ppbv in the HES), 0.76 ppbv for C₂H₂, 0.02 ppbv for C₆H₁₄, 1.12 ppbv for C₃H₈, and 1.07 ppbv for C₂H₄. The CH₄ seasonal difference of 21 ppbv

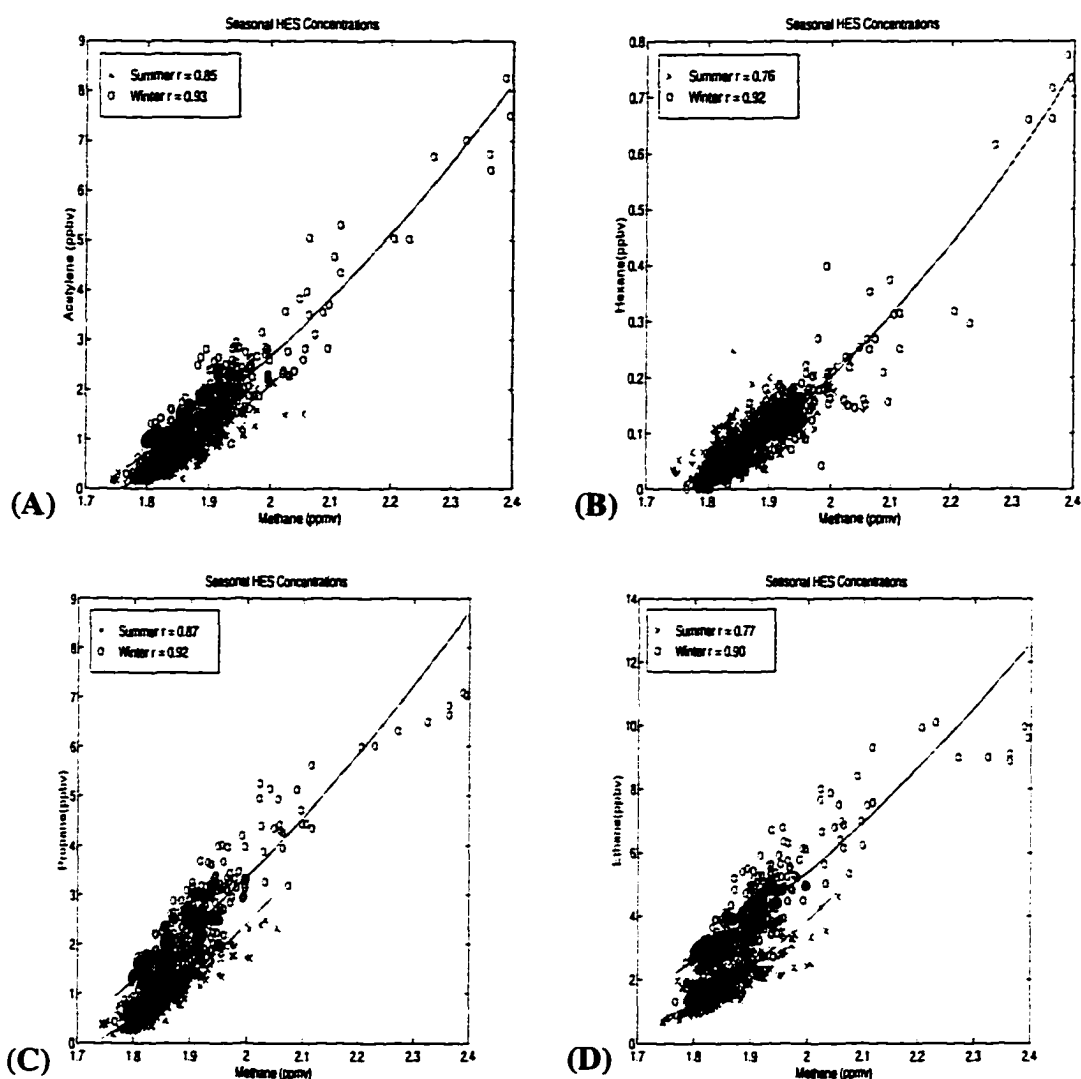


Figure 20: Methane plotted as a function of (a) acetylene, (b) hexane, (c) propane, and (d) ethane for the HES. Correlations between species are shown in the upper left of each figure. Data is fit by a least-squares algorithm.

compares to the background seasonal cycle that was found at the site when the lower 10-30% of each months data were used. Maximum mixing ratios for each species, especially in the winter, are much less than was observed in HES. For CH_4 the maximum winter mixing ratio is 1921 ppbv, about 550 ppbv lower than is observed in the HES. Correlations between species are much lower and indicate only a weak linkage between CH_4 and other

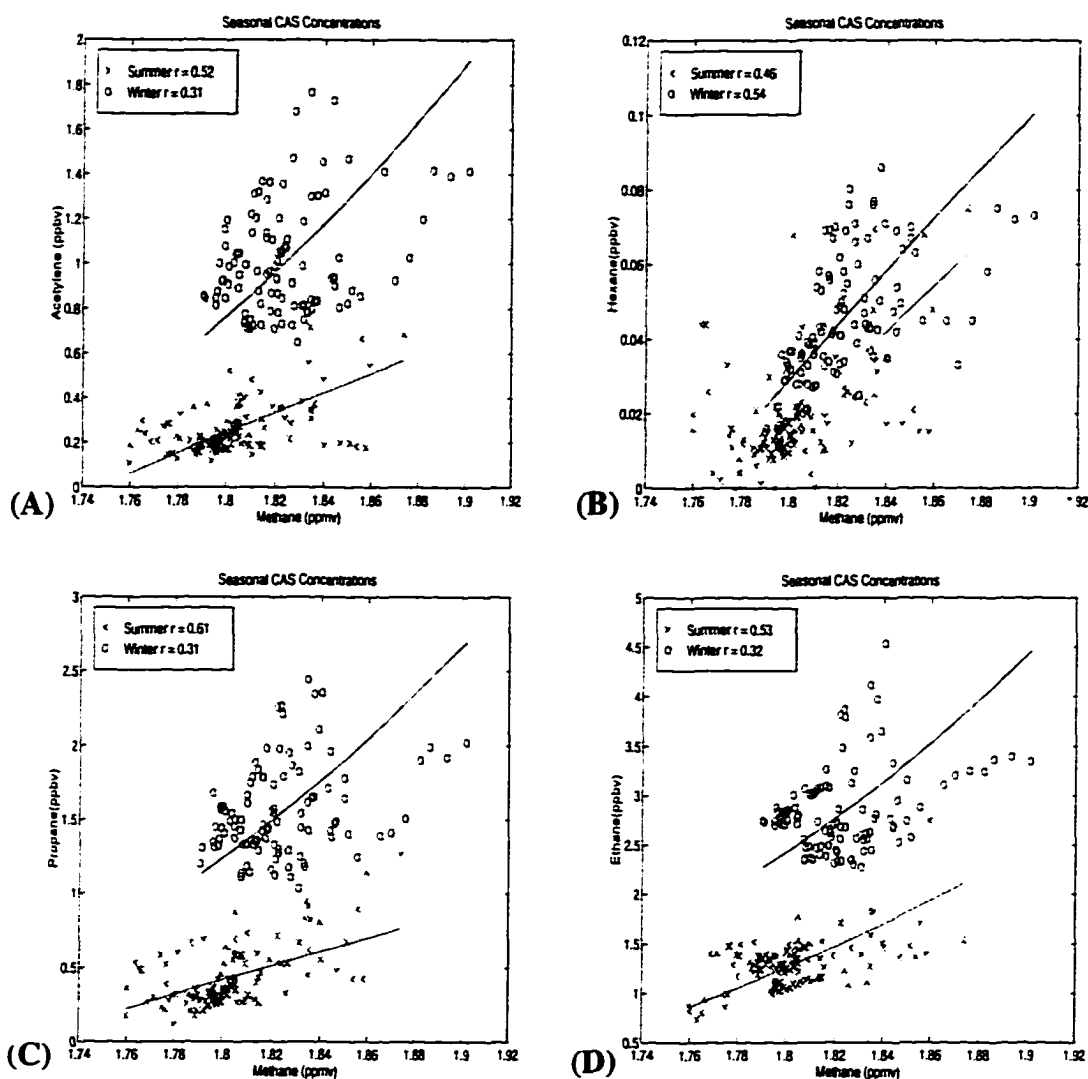


Figure 21: Methane plotted as a function of (a) acetylene, (b) hexane, (c) propane, and (d) ethane for the CAS.

species. The correlation between CH_4 and C_2H_2 is higher in the summer than the winter, 0.52 as compared to 0.31. This is opposite to the HES as the summer correlation is 0.85 and increases to 0.93 in the winter. CH_4 to C_3H_6 and C_2H_4 correlations behave in the same manner, decreasing from summer to winter in the CAS as compared to increases between seasons in the HES.

The differences in correlations between species in the CAS (weak) and HES

(strong) appear to be caused by a combination of distance from the site and emissions from different types of sources. The air originating from the CAS originates mostly from Canada or Maine, where wetlands are the dominant CH_4 source in the summer. During the winters, the primary source of CH_4 is from long range transport. Although wetlands are the strongest source in the New England region, their distance from the site and very infrequent winds from the CAS minimizes this strong seasonal source. In contrast, the HES is dominated by emissions from landfills year round, which are often advected to the site in association with the frequently occurring SW flow.

7.3 Worcester, MA. and Providence, RI.

The cities of Worcester, MA and Providence, RI. and two large landfills (Plainville and East Bridgewater) appear to be the sources of enhancements in chemical constituents at 120-140° (Figures 22 a-d). The mean winter minus summer mixing ratio is 37 ppbv for CH_4 , 0.94 ppbv for C_2H_2 , 0.04 ppbv for C_6H_{14} , 1.18 ppbv for C_3H_8 , and 1.71 ppbv for C_2H_4 .

The winter season correlations between CH_4 and other species is only slightly lower than that is observed in the HES ranging from 0.78 between CH_4 and C_2H_4 to 0.89 between CH_4 and C_6H_{14} . Summer correlations ranging from 0.43 between CH_4 and C_6H_{14} and 0.76 between CH_4 and C_3H_8 also lower as compared to the HES. Maximum CH_4 mixing ratios are also lower (2049 as compared to 2471 ppbv) indicating this sector is not subjected to as severe pollution events as those observed in the HES. Despite cities with similar populations and distances from the site, as well as large landfills in this quadrant, it appears that infrequent winds from the SE reduces the potential influences of these sources as compared to the HES.

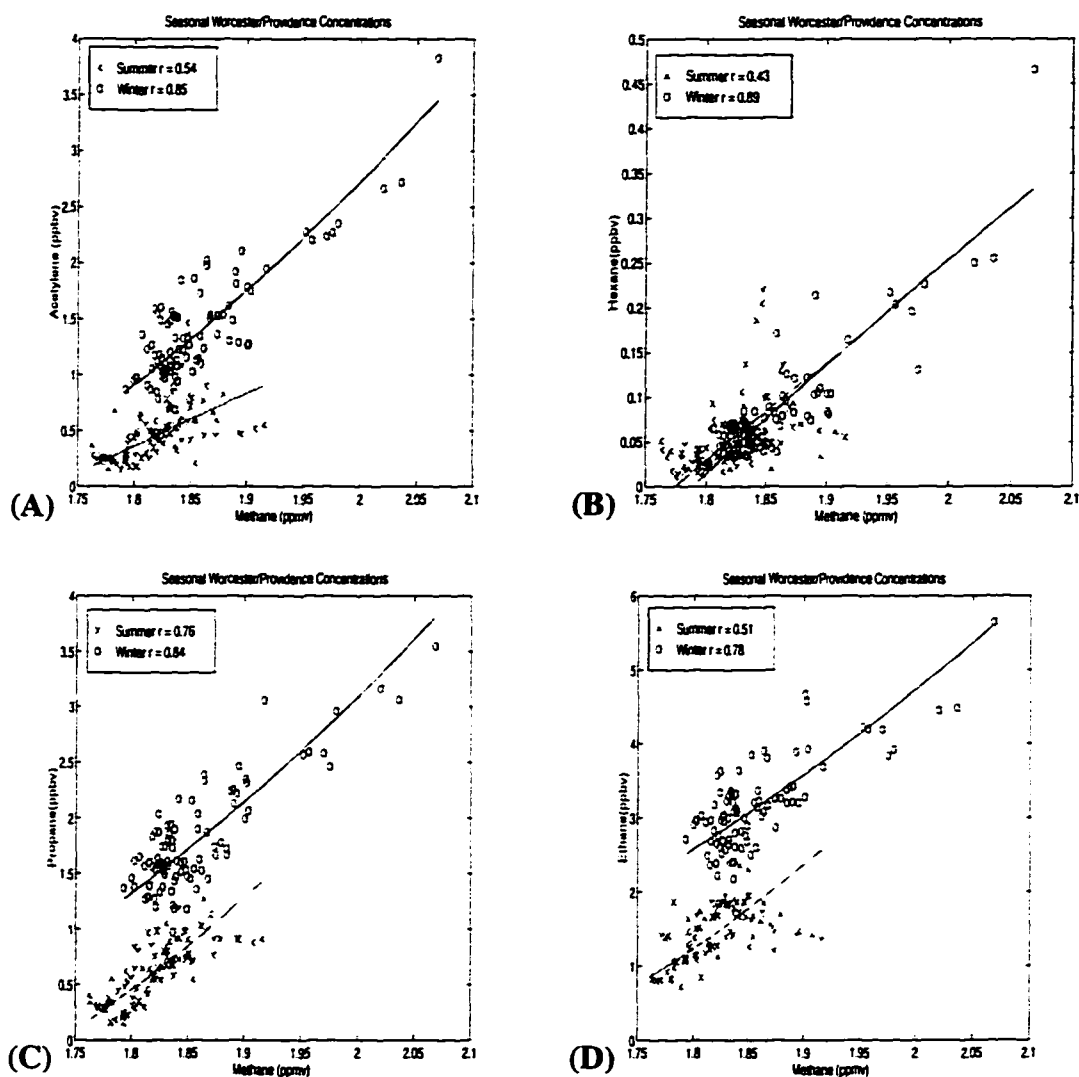


Figure 22: Methane plotted as a function of (a) acetylene, (b) hexane, (c) propane, and (d) ethane for Worcester, MA and Providence, RI.

7.4 Boston, MA.

The city of Boston, MA. appears to be the primary source of enhancements seen at 90 and 100° and includes emissions from one of three largest landfills in the region (Figures 23a-d). Mean winter minus summer differences are lower than the other quadrants being only 9 ppbv for CH₄, 0.43 ppbv for C₂H₂, 0.01 ppbv for C₆H₁₄, 0.60 ppbv for C₃H₈,

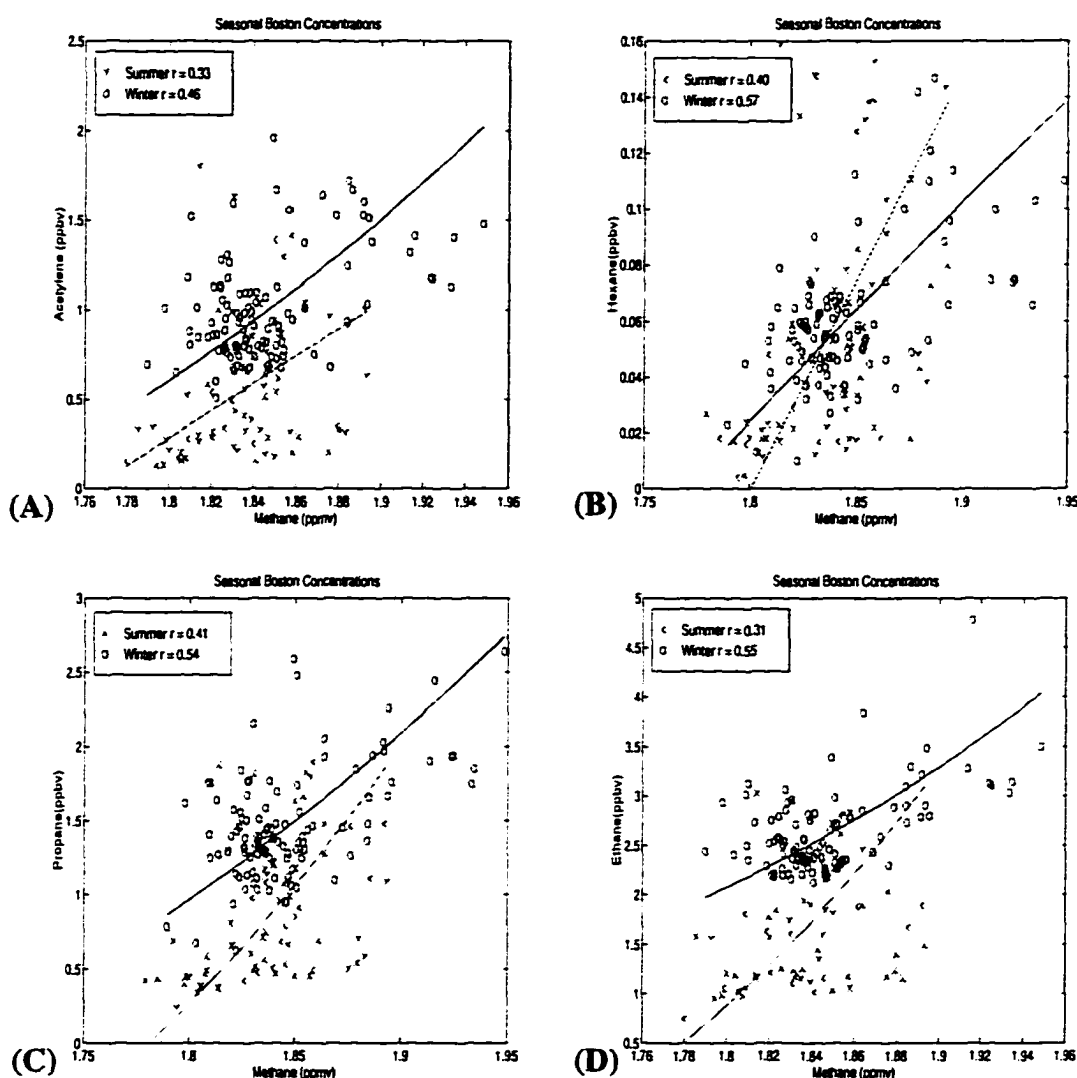


Figure 23: Methane plotted as a function of (a) acetylene, (b) hexane, (c) propane, and (d) ethane for Boston, MA.

and 0.93 ppbv for C_2H_4 . Summer means of species are higher than for PW and Petersham and are similar but still less than mean mixing ratios in the HES. Winter means are lower than PW and Petersham. The highest mixing ratios of species is much less as compared to the HES and similar to the PW quadrant.

The correlation between species is less than is observed for the HES, being around 0.40 in the summer and 0.55 in the winter. The longer distance from Boston to the site as

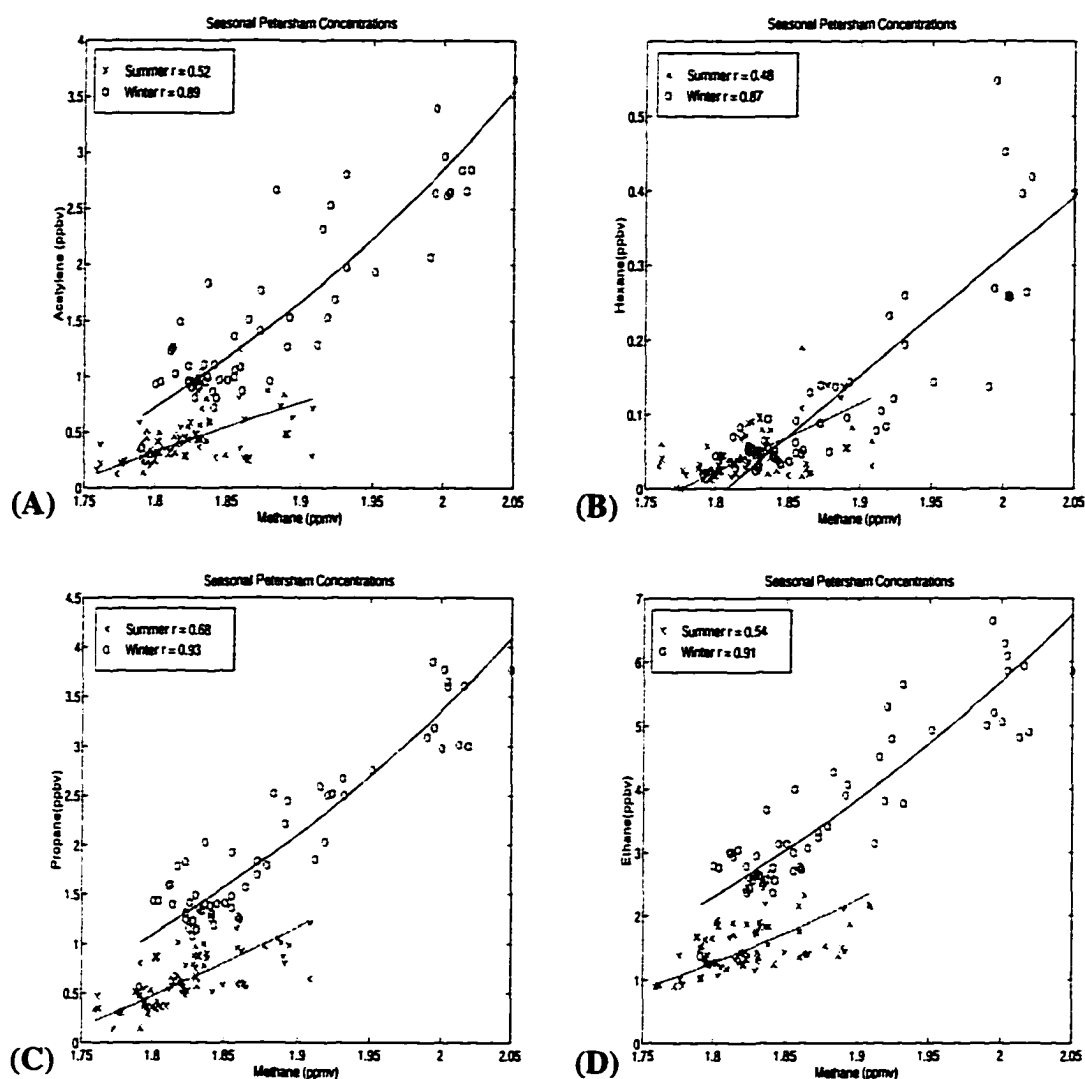


Figure 24: Methane plotted as a function of (a) acetylene, (b) hexane, (c) propane, and (d) ethane for Petersham, MA.

compared to the HES allows for more dilution of pollutants. Also, a persistent easterly flow advecting pollution to the site occurs less frequently than the dominant SW flow observed in the summer and at times in the winter.

7.5 Petersham, MA.

The small town of Petersham, MA., 6 km distant, appears to be the source of higher mixing ratios of CH_4 and other anthropogenic by-products at 170° (Figures 24 a-d).

The winter minus summer mixing ratio is largest in the Petersham sector including the HES and is 60 ppbv for CH_4 , 1.13 ppbv for C_2H_2 , 0.09 ppbv for C_6H_{14} , 1.36 ppbv for C_3H_8 , and 2.14 ppbv for C_2H_4 . Summer mixing ratios are similar to PW and winter values are close to those observed in the HES.

The correlation between species is high in the winter with values around 0.9, similar to the HES. However summer values are lower, around 0.5, which is less than the HES and is similar to PW. Higher maximum mixing ratios of species are seen in this quadrant than as compared to Boston or Providence.

The ratio of C_3H_8 and C_2H_4 can be used to discriminate between wood burning or LPG as the likely source for the local enhancements. A C_3H_8 to C_2H_4 ratio of .3-.5 implies wood burning, while values closer to 1 are related to sources of LPG. Ratios range from .4 to .6, so wood burning for home heating appears to be causing these rather large winter time enhancements. Terrain effects may be enhancing the effects of Petersham pollutants in the measurements by channeling emissions from close by sources to the tower.

7.6 Site Sensitivities

The critical factors influencing the magnitude of chemical enhancements at the site are: Proximity of sources, predominant wind direction, source strengths/population size, and terrain effects. The effects of wood burning in Petersham show up very strongly due to the close proximity of the town, perhaps enhanced by terrain effects. Conversely, the larger town of Athol (7 km distant at 329°) with a population of 11 thousand does not show up as a strong source even though it is as close and winds are from 330° as often as they are from 170° . Perhaps the increased mixing associated with gusty NW winter winds in combination with terrain effects is mixing or channeling pollution around or over top of

the sampling location.

The strongest known anthropogenic CH₄ sources are not causing the largest enhancements because their emissions reach the site infrequently. The three largest landfills closest to HF are located in the 90 and 120-130° wind quadrants at distances of 89-113 km. While enhancements in those quadrants are at least in part due to these landfills it appears that their distance from the site in combination with an infrequent wind flow from those directions minimizes their impact as compared to multiple smaller sources in the HES that are closer to the site.

In the CAS, emissions from wetlands that are known to be the dominant source in the summer are only very weakly seen at the site if at all. This would be do to a combination of distance and very limited wind flow from that quadrant.

7.7 Yearly Changes in the HES and CAS

Examining the chemical composition of the HES and CAS year by year provides additional insight as to how the composition of the air sampled may be changing over time. Extreme values of both CH₄ and C₂H₂ are seen in all years, especially 1994 and 1995. Year to year variability is quite pronounced and additional years of data will be needed to determine any definitive trends. Table 9 provides summary statistics on a yearly basis for a CH₄ and C₂H₂.

Winter CH₄ and C₂H₂ mixing ratios for the HES and CAS are plotted in Figures 25 a-d. The mean value of CH₄ in the HES increases from 1866 to 1913 ppbv, while the mean value of C₂H₂ increases from 1.43 to 1.62. Correlations between CH₄ and C₂H₂ in the HES are consistently high increasing from .89 in 1993 to .98 in 1995. The mean value of CH₄ in the CAS increases from 1818 to 1847 ppbv. Correlations between CH₄ and

Table 9: Yearly Summary Statistics for the CAS and HES

Year	Winter				Summer			
	CAS		HES		CAS		HES	
	mean	std	mean	std	mean	std	mean	std
Methane (ppbv)								
1992	1818	10	1866	67	1784	12	1853	53
1993	1814	17	1843	42	1779	12	1827	37
1994	1820	11	1910	73	1803	18	1860	53
1995	1847	24	1913	114	1807	23	1836	35
Acetylene (ppbv)								
1992	no data	no data	no data	no data	.26	.16	.85	.52
1993	1.16	0.25	1.43	.52	.24	.76	.66	.36
1994	0.89	0.13	1.84	.88	.25	.13	.78	.45
1995	0.91	0.22	1.62	1.38	.27	.11	.55	.27

C_2H_2 in the CAS are more variable and lower than those in the HES being .76, .39, and .91 for 1993-1995 respectively. The larger variability in correlations is due to longer range transport and may be due to yearly emission changes from wetlands due to temperature and precipitation changes from year to year.

Summer CH_4 and C_2H_2 mixing ratios for the HES and CAS for CH_4 are shown in Figures 26 a-d. The mean values of CH_4 and C_2H_2 in the HES are variable from year to year, ranging from 1827-1860 ppbv for CH_4 and .55 to .85 for C_2H_2 . Correlations between CH_4 and C_2H_2 in the HES remain uniformly high being .97, .88, .83, and .83 for 1992-1995 respectively. The mean value of CH_4 in the CAS increases from 1784 in 1992 to

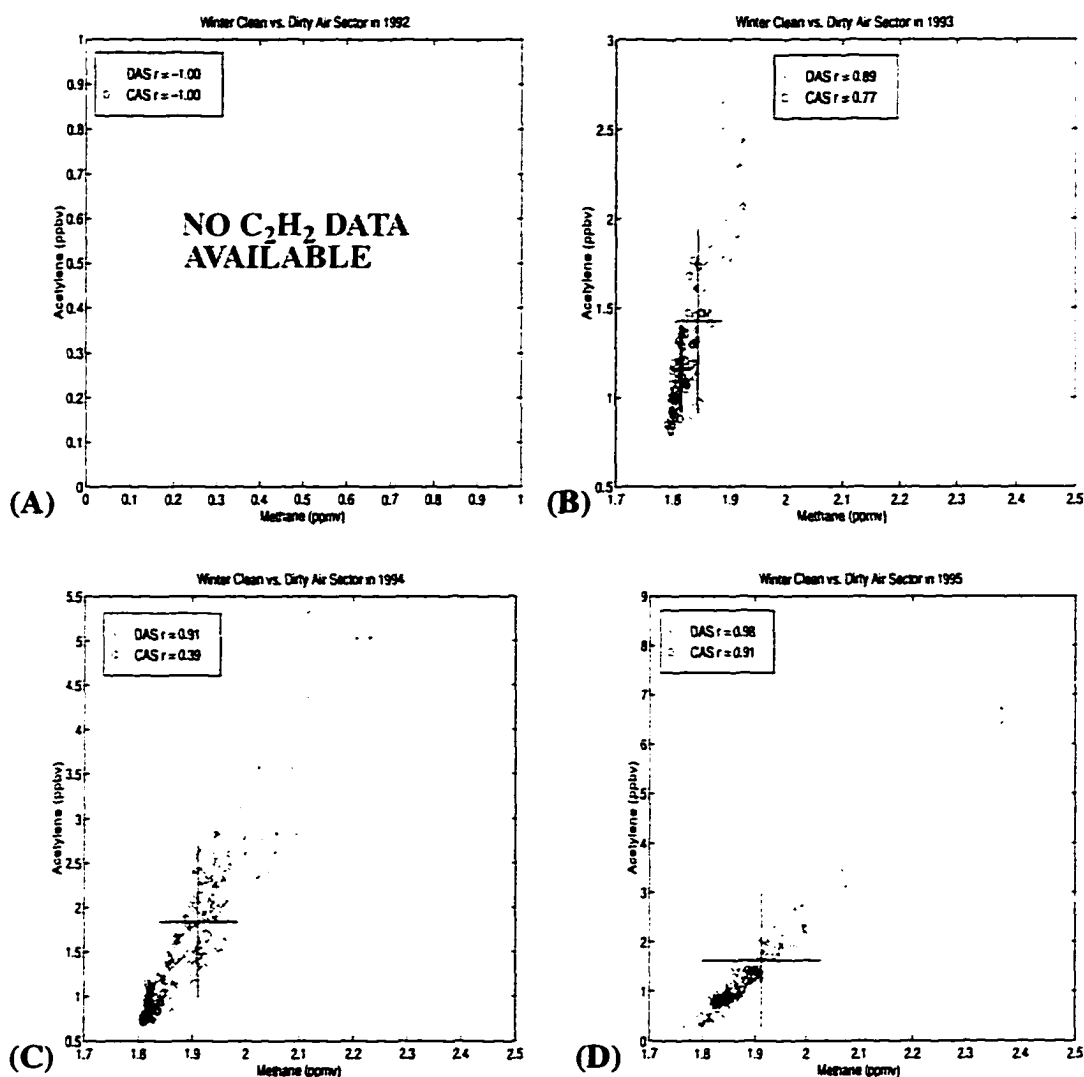


Figure 25: Winter methane and acetylene for the HES and CAS for years 1993 - 1995 (a-d). The cross bars are the mean and ± 1 standard deviation for each species as a function of season.

1807 ppbv in 1995. Correlations between CH_4 and C_2H_2 in the CAS are .46, .80, and .41 for the years 1993-1995.

Differences between the CAS and HES in the first and last year of the study may be used to examine the trend. From 1992 to 1995, CH_4 increases 29 ppbv in the winter CAS and 23 ppbv in the summer CAS. This compares favorably to the 5.5 ± 2 ppbv that

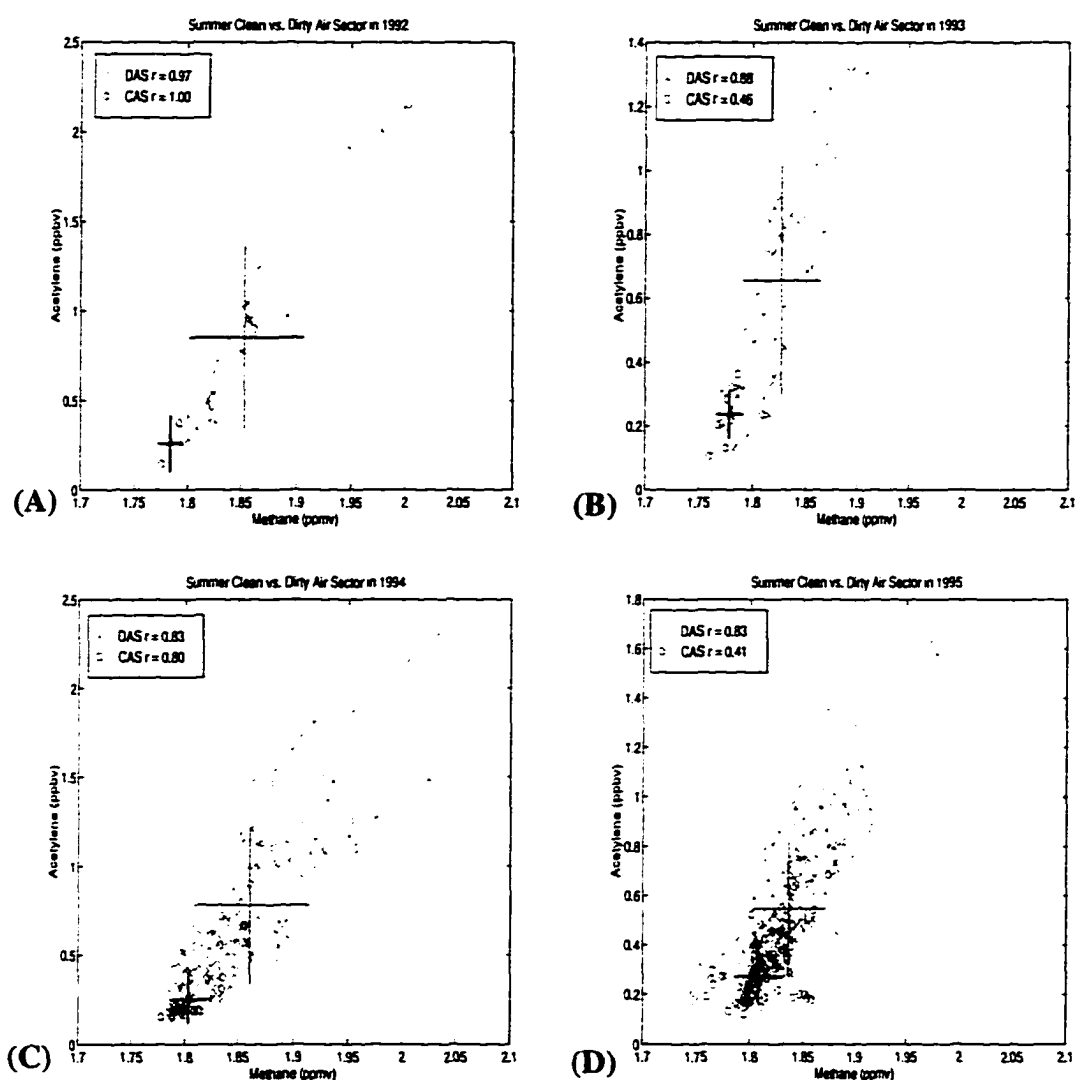


Figure 26: Summer methane and acetylene for the HES and CAS for years 1992 - 1995 (a-d).

was found in a subset of the full data set that was considered background air. CH_4 mixing ratios increase from 1866 to 1913 in the winter HES, while the summer HES declined 17 ppbv from 1853 to 1836 ppbv.

CHAPTER VIII

CASE STUDIES

Three case studies demonstrate how enhancements in particular transport pathways described above in the mean yearly and seasonal flow regimes occur. Of particular interest is to determine if emissions from strong sources reach the site on a regular and repeatable basis.

8.1 Criteria / Grouping

The beginning of a high CH₄ event is defined when mixing ratios exceed the monthly median + MAD for a time period greater than 2.4 hours. The events, numbering 377 for the 4 year time period, can be broken into three broad categories: the first is a build up of CH₄ during the overnight hours, due mostly to nocturnal temperature inversions. These events are relatively short lived (12 hours or less) and make up 49, 58, 47, 46% of the cases. The second category is caused by the advection of pollution by regional/local transport in which a rapid increase (≥ 200 ppbv/hr) of CH₄ mixing ratios is observed. These events are closely linked to a persistent wind flow from strong source regions, primarily large landfills in the case of CH₄ and cites for other anthropogenic species. The third category is the combination of types 1 and 2, where pollution from local and regional sources is advected to the site while being trapped at the surface for an extended period of time by a strong temperature inversion which can persist for days.

There is no trend in the number of events observed during the four year time period. Overall, 1993 had the most total events with 123, 1992 the lowest with 79 (due in

part to limited data for the winter time period). For events lasting more than one day, 1993 had the most with 24 and 1994 the least with 15. The number of total events between seasons on a year to year basis also varies considerably. The season with the highest number of total events was different for each of the four years. However, for events ≤ 1 day, the spring and summer seasons have the most, while for events ≥ 1 day, the winter and fall seasons have consistently more episodes than the spring and summer seasons.

The case studies, when grouped by the prevailing wind direction, are found to fall into wind quadrants similar to sectors previously described by enhancements in the mean flow fields. The largest number of pollution events (42%) occurred in the SW quadrant, primarily during the winter seasons. This is linked to the prevalent synoptic pattern in which warmer air is transported over the colder ground surface trapping pollutants near the surface. Other cases occurred much less frequently with flow from the SE (10%) and east (7%) being the second and third category of grouped events. A persistent flow with enhancements of CH_4 from other directions was rare. Some of the cases could not be classified due to a complex or changing wind regime in which the path of the air mass was not evident (22%) and an additional category for summer time stagnation events was also included when winds remained light and variable for more than a day (12%).

8.2 Case study 1: 17- 20 February, 1994

This case examines polluted SW flow and contains the highest mixing ratios of CH_4 recorded during the study period. Figures 27 (a-f) depict CH_4 , C_2H_2 , C_6H_{14} , ratio of C_3H_8 and C_2H_4 , wind direction, and wind speed for the three day period 17-20 February 1994. Two significant peaks in CH_4 are observed near 8 PM on 17 and 19 February, with values falling thereafter through the night and reaching a minimum during the late after-

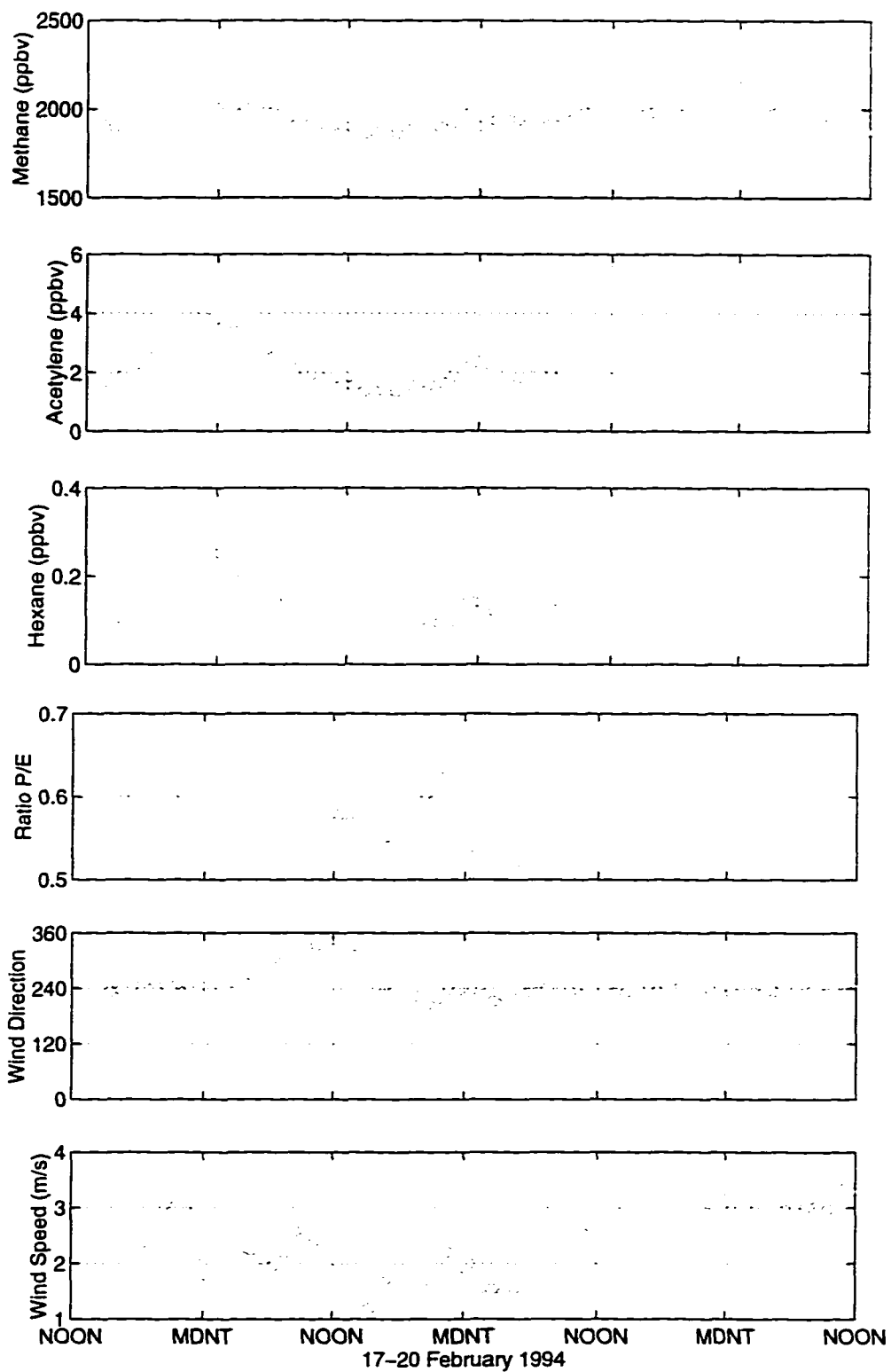


Figure 27: Methane, acetylene, hexane, ratio of pentane and ethane, wind direction, and speed for 17-20 February, 1994.

noon. The maximum mixing ratio is 2471 ppbv, with a median value of 1949 ppbv for the three day period, an enhancement of 109 ppbv over the monthly median. For the data that was available, the correlation between CH_4 and C_2H_2 is .96, CH_4 and C_6H_{14} is .92, CH_4 and C_2H_4 is .81.

The critical circumstances leading to this event are a persistent SW flow advecting pollution from nearby sources to the site. The wind direction is from the SW for over 48-hours, with a brief shift to the west/NW at the beginning of the event, while the wind speed is 2-3 m/s during the day and nearly calm at night. The nearby Worcester, MA. sounding depicted a strong temperature inversion at 500 m which would further limit mixing. As warmer air associated with the SW flow moved over the snow covered ground it is likely shallow stable layers trapped pollutants, including smoke from fires, close to the ground. Two landfills, Chicopee (51 km distant) and Granby (37 km distant) are most likely the source of these CH_4 emissions. The cities of Springfield and Northampton, MA. are the probable source of the other anthropogenic pollutants. Trajectories at six hour intervals track the tower winds and show the air passing near the city of Springfield about six hours prior to reaching the site. As important is that the trajectories do not show transport from any other metropolitan areas, especially New York as the trajectory paths pass inland in a more westerly direction by several hundred miles.

8.3 Case study 2: 13-14 January 1995

This case is similar to the one above as SW flow again advects pollution from regional sources to the site (Figures 28 a-f). The maximum CH_4 mixing ratio of 2.467 ppmv, the highest observed in 1995, was observed between 9 PM and 1 AM overnight on 13-14 January, 1995. The median mixing ratio for the event was 2031 ppbv, which repre-

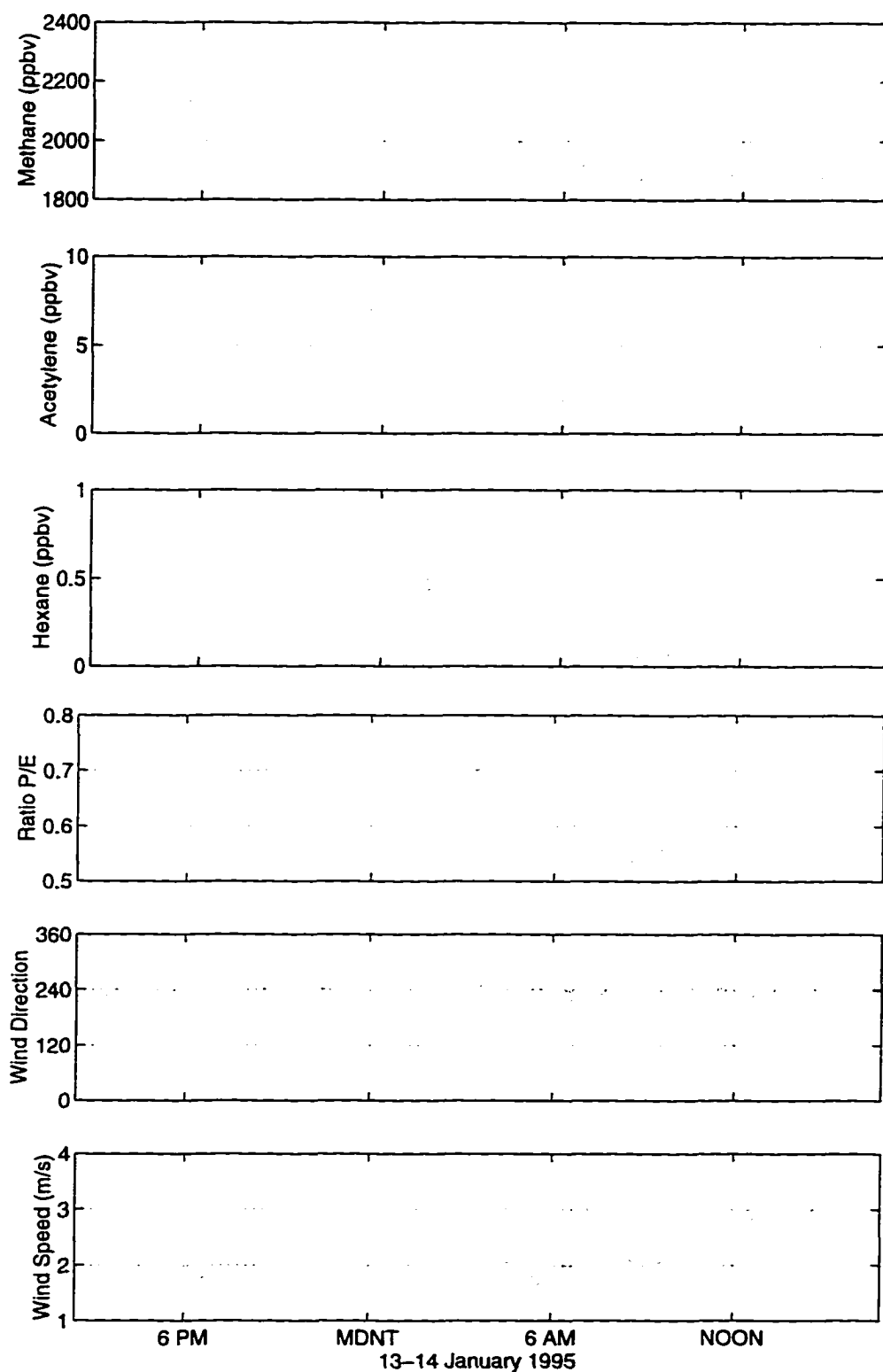


Figure 28: Methane, acetylene, hexane, ratio of pentane and ethane, wind direction, and speed for 13-14 January, 1995.

sents a 190 ppbv increase over the background levels. Correlations between species are again very high being .99 for CH_4 and C_2H_2 , .99 for CH_4 and C_6H_{14} , and .98 between CH_4 and C_2H_4 .

Similar circumstances of a persistent SW wind advecting pollution from strong regional sources combined with limited vertical mixing traps pollutants near the surface, especially during the over night hours. The wind direction is from the SW, while the wind speed is generally less than 2 m/s until near the end of the event. Trajectories show the path of the air parcels backing over time with air initially surging northward across Long Island, then across New York City and then passing Springfield before reaching the site. Due to the freshness of the signature and an estimated transport time in excess of two days from the New York metropolitan area to the site it appears that similar to the case above that it is strong local emissions rather than the more distant sources that are causing these severe pollution events at the site.

8.4 Case study 3: 6 August 1992

This case examines a south-to SE flow which appears to be maritime air that picked up CH_4 prior to reaching to site from strong regional sources (Figures 29 a-f). The maximum mixing ratio of CH_4 was 1866 ppbv, the median mixing ratio for the event was 1830 ppbv, which represents a 29 ppbv increase over the monthly median. Unlike the previous two case studies, the species are anti-correlated with CH_4 and have correlations of -0.46 between CH_4 and C_2H_2 , -0.41 for CH_4 and C_6H_{14} , and .13 between CH_4 and C_2H_4 . The wind speed averages 1.3 m/s for the twenty-four hour period. Trajectories move the air parcels in a near northerly direction off the Atlantic across the lightly populated inte-

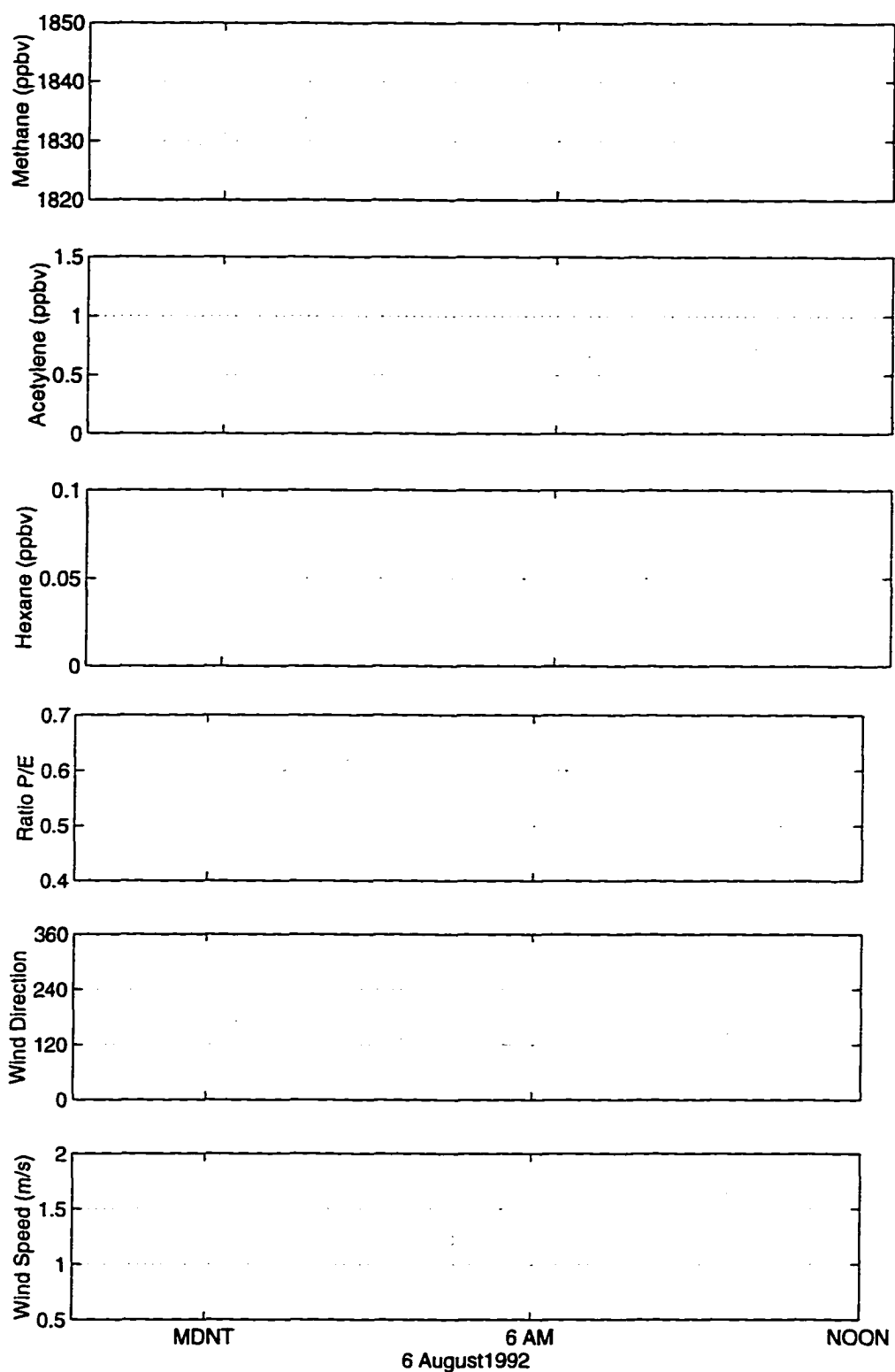


Figure 29: Methane, acetylene, hexane, ratio of pentane and ethane, wind direction, and speed for 6 August 1992.

rior sections of Rhode Island. Just prior to reaching the site the air passes over a nearby landfill in Barre 10 km distant.

CHAPTER IX

CONCLUSIONS

For the years 1992-1995 approximately 125,000 individually measured CH₄ mixing ratios were obtained at the HF research site. Over the 4-year period a variable upward trend of 5.5 ± 2 ppbv/year was observed in the background data. Comparison of changes in the full and background data sets suggest that there has been little change in anthropogenic CH₄ inputs at the sampling site during the 4-year time period.

The trend and seasonal cycle were found to be similar to the global data set when the effects of pollution were minimized by analyzing a subset of the data. This is significant as the global behavior of CH₄ is based on data that has been collected in remote regions carefully chosen to avoid the effects of pollution. Future sites could be located in more accessible and cost effective locations and can serve a dual purpose in characterizing both changes in the composition of clean, background air and changes in the number and severity of pollution events on a regional scale.

The seasonal cycle reaches a maximum in mid-winter and minimum in early summer. In the background data seasonal differences are around 25 ppbv, similar to that found for the global data set. Pollution events exaggerate the full data seasonal cycle, especially during the winter when stable atmospheric conditions appear to contribute to longer and more severe pollution events.

A daily cycle is observed in which maximum mixing ratios are observed just prior to sunrise and minimum mixing ratios in the afternoon near the time of maximum atmo-

spheric mixing. Cycles vary between seasons, having the largest amplitudes in late spring and early summer when local wetlands may contribute to the signal and again in the winter when emissions from wood burning for home heating may impact the site. Smallest changes are in the spring and fall from inputs from both wetlands and wood burning are low.

The HF research site sampled air flow from a variety of source regions. The proximity of cities allowed the chemical signature of the tower to be examined and the effect of pollution evaluated on time scales ranging from years to hours. The influence of pollution is particularly strong in the SW wind quadrant which encompasses an area that includes the combined inputs from Springfield, Northampton, and Amherst, MA. Pollution from other cities including Boston, MA. and Providence., RI also impacts the site. The near by town of Petersham south of the site leaves a strong signature in the winters which appears to be due to wood burning. Local sources are found to be the primary cause of the highest CH₄ events, with regional and perhaps more distant sources elevating the background mixing ratios, especially in the heavily populated SW wind quadrant.

CH₄ is strongly correlated to C₂H₂, C₆H₁₄, and C₂H₄ in most cases and reflects the co-location of landfills and cities. On a seasonal basis correlation coefficients are generally greatest in the winters when the combination of increased wind speed and more prevalent temperature inversions reduces atmospheric mixing. Conversely in the summer seasons more vigorous vertical mixing and weaker and less frequent temperature inversions allow for better mixing of constituents. As a function of wind direction correlations between CH₄ and C₂H₂ are tightest in the HES where a fresh signal from the many near by sources is observed and are the lowest in the CAS where generally clean, aged air is sampled.

Case studies show that strong regional sources can be related to the most severe pollution events. Critical to these high episodes is the combination of a light and persistent wind and stable atmospheric conditions which then allows pollution to be advected to the site with very little mixing. Landfills in the SW quadrant are thought to contribute to highest recorded values at the site.

Future work will incorporate additional years of data that are still being collected and will analyze in more detail other case studies and additional chemical species to further understand and partition local, regional, and distant transport to the site.

APPENDIX A: POSSIBLE SOURCES OF ERROR

Table 10 attempts to capture the major sources of error / variation that I have encountered in this research effort. Error as defined in Websters Dictionary is the “difference between an observed or calculated value and a true value; variation in measurements, calculations, or observations of a quantity due to mistakes or to uncontrollable factors”. The table contains three columns with the first column listing the source of the error. Column 2 is the potential severity of the error where 1 is minor and 5 is major. Column 3 is my ability to reduce or eliminate the source of error in column 2. Values again range from 1 (I can virtually eliminate the error) to 5 (I can do nothing about the error).

Quality assurance and quality control (QA/QC) are an important part of any scientific understanding. This research effort used data from differing temporal and spacial resolutions in an attempt to identify CH₄ cycles and trends in the Northeastern part of the United States. At each step along the way possible sources of errors were identified and if possible reduced.

ANALYTICAL SYSTEMS:

Details for the CH₄ system are given in the body of the dissertation. Other chemical and meteorological data that I used are also collected at the same site, but by different research groups and at differing time resolutions. I was given hourly averaged values for all species that I used and had to create hourly mean mixing ratios for the CH₄ data in order to be able to compare them.

Instrument failures occur for a variety of reasons (lightening strikes, wind damage, mechanical failure) and tend to last for extended time periods when they do occur. These

data gaps propagate down as significant potential source of error when data merging and analysis steps begin.

HUMAN INTERACTIONS

Once the raw data are collected the “human” factor comes into play allowing the potential of a variety of errors of differing severity to be introduced. I (and others) spent extensive amounts of time in QA/QC for the CH₄ data set. Different kinds of screening were used to check for simple things such as incorrect times or values that were out of range. Data shifts which occurred when gas standards were changed were easily detected and corrected. More sophisticated checking involved looking at how fast the data changed over differing time periods and flagging suspicious data. Unfortunately this is somewhat of a subjective type process as what constitutes “bad” data is not explicitly defined.

RELATING POINT AND SPATIAL DATA

Thus far all the data sets I have mentioned have been collected at one site representing a single point in central Massachusetts. I also used other data including locations and estimates of CH₄ emissions from landfills and wet lands, use of meteorological data from surrounding locations, use of National Meteorological Center grided data, and the use of air mass backward trajectory analysis. Similar to the point data, spacial data errors occur in many forms and are summarized below.

(1) Estimation errors: The data from meteorological grids had to be horizontally and vertically interpolated to the point site.

(2) Variability/changes in sources over time: Wet lands are a source of CH₄ primarily in the last spring and early summer. Wood burning for home heating is a minor but important source only in the winter and early spring.

(3) Assumption of straight line winds: Enhancements in chemical species are related to cities in the same wind sector. This would not be the case for long range transport, but is a reasonable assumption for the mean flow.

(4) Estimation of species lifetimes: This is a very rough estimate. Unfortunately it is not possible to know cloud conditions along the path of the air parcel. This is further complicated by the errors in wind speed, direction, and back trajectory paths. However using species with different lifetimes to put upper and lower bounds on the age of the air, combined with trajectories is a powerful method to define the age of the pollutants being sampled.

(5) Site sensitivities: With a single point one can account for the effects of terrain which may lead to some source being either over or under represented as seem to be the case for Petersham (over) and Athol (under). Also one cannot determine the effects of multiple sources that may stack up pollutants prior to the time they reach the site.

SUMMARY

I have tried to identify and account for as many sources of error as possible. Extensive time was spent on QA/QC on the raw CH₄ data set and that was the emphasis of this research. Appropriate statistical techniques were used to analyze this data set which was non-normally distributed and contained large data gaps.

Table 10: Sources of Potential Error

Error Source	Error Contribution Potential	Correctable
	1=LOW 5=HIGH	1=YES 5=NO
Analytical Systems		
Measurement uncertainties of CH ₄ instrument	1	2
Measurement uncertainties in other data	2	4
Data gaps	3	5
Human Interactions		
QA/QC of the CH ₄ data	2	2
QA/QC of other data	4	3
Obvious errors/inconsistencies	5	1
Data processing and merging		
Interpolation of raw CH ₄ data to other time periods	2	2
Determination of use of proper time length	3	3
Use of other averaged data sets	4	4
Proper choice of mathematical/statistical techniques	3	1
Relating point and spatial data		
Variability of sources	3	5
Assumption of straight line winds	3	5
Calculation of species life times	2	3
Site Sensitivities	5	5

LIST OF REFERENCES

- Blaha, D., K. Bartlett, P. Czepiel, R. Harriss, and P. Crill, Natural and Anthropogenic Methane Sources in New England., in review.
- Blake, D. R. and F. S. Rowland, Continuing worldwide increase in tropospheric methane, 1978 to 1987, Science, Vol. 239, pp. 1129-1131, 1988.
- Blake D. R., N. J. Blake, T. Smith, O. Wingenter, and F. S. Rowland, Nonmethane Hydrocarbon and Halocarbon Distributions During Atlantic Stratocumulus Transition Experiment/Mane Aerosol and Gas Exchange, June 1992, J. Geophys. Res., Vol 101, No. D2, pp. 4,501-4,514, 20 February, 1996.
- Blake, N. J., D. R. Blake, B.C. Sive, T. Chen, and F. S. Rowland, Biomass burning emissions and vertical distribution of atmospheric methyl halides and other reduced carbon gases in the South Atlantic region, J. Geophys. Res., Vol 101, No. D19, pp. 24,151-24,164, 30 October, 1996.
- Bogner, J., K. Spokas, E. Burton, R. Sweeney, and V. Corona, Landfills as atmospheric methane sources and sinks, Chemosphere, Vol. 31, No. 9, pp. 4119-4130, 1995.
- Brook J., P. Samson, and S. Silman, A Meteorology-Based Approach to Detecting the Relationship between Changes in SO₂ Emission Rates and precipitation Concentrations of Sulfate., Journal of Appl. Meteo., Vol 33, No. 9, pp. 1050-1066, 1994.
- Brook J., P. Samson, and S. Silman, Aggregation of Selected Three-Day Periods to Estimate Annual and Seasonal Wet Deposition Totals for Sulfate, Nitrate, and Acidity. Part I: A Synoptic and Chemical Climatology for Eastern North America., Journal of Appl. Meteo., Vol 34, No. 2, pp. 297-325, 1995.
- Chappellaz, J., J. M. Barnola, D. Raynaud, Y. S. Korotkevich, and C. Lorius, Ice-core record of atmospheric methane over the past 160,000 years, Nature, Vol. 345, pp. 127-131, 10 May, 1990.
- Conway, T. J., P. P. Tans, L. S. Waterman, K. W. Thoning, D. R. Kitzis, K. A. Masarie, and N. Zhang, Evidence for interannual variability of the carbon cycle from the NOAA/CMDL Global Air Sampling Network, J. Geophys. Res., Vol. 99, No. D11, pp. 22,831-22,855, 20 November, 1994.

- Czepiel, P. M., B. Mosher, R. C. Harriss, J. H. Shorter, J. B. McManus, C. E. Kolb, E. Allwine, and B. K. Lamb, Landfill methane emissions measured by enclosure and atmospheric tracer methods, J. Geophys. Res., Vol. 101, No. D11, pp. 16,711-16,719, 20 July, 1996A.
- Czepiel, P. M., B. Mosher, P. M. Crill, and R. C. Harriss, Quantifying the effect of oxidation on landfill methane emissions, J. Geophys. Res., Vol. 101, No. D11, pp. 16,721-16,729, 20 July, 1996B.
- Danielsen, E. F., Trajectories: Isobaric, isentropic and actual, J. Meteorol., 479-486, 1961.
- Dlugokencky E. J., L. P. Steele, P. M. Lang, and K. A. Masarie, The growth rate and distribution of atmospheric methane, J. Geophys. Res., Vol. 99, No. D8, pp. 17,021-17,043, 20 August, 1994A.
- Dlugokencky E. J., K. A. Masarie, P. M. Lang, P. P. Tans, L. P. Steele, and E. G. Nisbet, A dramatic decrease in the growth rate of atmospheric methane in the northern hemisphere during 1992, Geophys. Res. Lett., Vol. 21, pp. 45-48, 1994B.
- Etheridge, D. M., G. I. Pearman, and P. J. Fraser, Changes in tropospheric methane between 1841 and 1978 from a high accumulation-rate Antarctic ice core, Tellus, Vol. 44B, pp. 282-294, 1992.
- Frolking, S. and P. Crill, Climate controls on temporal variability of methane flux from a poor fen in southeastern New Hampshire: Measurement and modeling, Global Bio. Cycling, Vol. 8, No. 4, pp. 385-397, December, 1994.
- Fung I., John J., Lerner J., Matthews E., Prather M., Steele L. P., and Fraser P. J.: Three-dimensional model synthesis of the global methane cycle. J. Geophys. Res., Vol 96, No. D7, pp. 13,033-13,065, July 20, 1991.
- Gaines S. D. and Denny M. W., The largest, smallest, highest, lowest, longest, and shortest: Extremes in ecology, Ecology, Vol. 74, No. 6, pp. 1677-1692, 1993.
- Goldstein, A. H., B. C. Daube, J. W. Munger, and S. C. Wofsy, Automated in-situ monitoring of atmospheric non-methane hydrocarbon concentrations and gradients, J. of Atmos. Chem., Vol. 21, pp. 43-59, 1995A.
- Goldstein, A. H., S. C. Wofsy, and C. M. Spivakovsky, Seasonal variations of nonmethane hydrocarbons in rural new england: Constraints on OH concentrations in northern mid-latitudes, J. Geophys. Res., Vol. 100, No. D10, pp. 21,023-21,033, 20 October, 1995B.

- Graedel T. E. and J. E. McRae, On the Possible Increase of the Atmospheric Methane and Carbon Monoxide Concentrations During the Last Decade., Geophys. Res. Lett., Vol. 7, No. 11, pp. 977-979, November 1980.
- Haagenzen, P. L. and M. A. Shapiro, Isentropic Trajectories for derivation of objectively analyzed meteorological parameters, Tech. Note *NCAR/TN-149*, 30 pp., Natl. Cent. for Atmos. Research, Boulder, Colo., 1979.
- Harris J. M., P. P. Tans, E. J. Dlugokencky, K. A. Masarie, P. M. Lang, S. Whittlestone, and L. P. Steel, Variations in atmospheric methane at Mauna Loa observatory related to long-range transport, J. Geophys. Res., Vol. 97, No. D5, pp. 6,003-6,010, 20 April, 1992.
- Hirsch, A. I., Munger J. W., Jacob, D. J., Horowitz, L. W., and A. H. Goldstein, Seasonal variation of the ozone production efficiency per unit NO_x at Harvard Forest, Massachusetts, J. Geophys. Res., Vol 101, No. D7, pp. 12,659-12,666, 20 May, 1996.
- Holzworth, G. C., Mixing depths, wind speeds and air pollution potential for selected locations in the United States., Journal of App. Meteorology., Vol. 6, pp. 1039-1044, 1969.
- Intergovernmental Panel on Climate Change, Climate Change: The IPCC Scientific Assessment, 365 pp., Cambridge Univ. Press, New York, 1990.
- Intergovernmental Panel on Climate Change, Climate Change 1992: The Supplementary Report to the IPCC Scientific Assessment, 200 pp., Cambridge Univ. Press, New York, 1992.
- Intergovernmental Panel on Climate Change: Climate Change 1994: Radiative Forcing of Climate Change and An Evaluation of the IPCC IS92 Emission Scenarios, 339 pp., Cambridge Univ. Press, New York, 1995.
- Keeling, C. D., T. P. Whorf, M. Wahlen, and J. van der Plicht, Interannual extremes in the rate of rise of atmospheric carbon dioxide since 1980, Nature, Vol. 375, pp. 666-670, 22 June, 1995.
- Khalil, M. A. and R. A. Rasmussen, Decreasing trend of methane: Unpredictability of future concentrations, Chemosphere, Vol. 26, Nos. 1-4, pp. 803-814, 1993A.
- Khalil M. A., R. A. Rasmussen, and F. Moraes, Atmospheric methane at Cape Meares: Analysis of a high-resolution data base and its environmental implications, J. Geophys. Res., Vol. 98, No. D8, pp. 14,753-14,770, 20 August, 1993B.
- Khalil, M. A. and F. Mores, Spectral analysis of time series, Rep. 93-61, Oregon Graduate Institute, Portland, OR., 1993C.

- Khalil, M. A. and R. A. Rasmussen, Global emissions of methane during the last several centuries, Chemosphere, Vol. 29, No. 5, pp. 833-842, 1994.
- Lang, P. M., L. P. Steele, R. C. Martin, and K. A. Masarie, Atmospheric methane data for the period 1983-1985 from the NOAA/CMDL global cooperative flask sampling network, Tech. Mem., ERL CMDL-1, NOAA, Boulder, CO., 1990A.
- Lang, P. M., L. P. Steele, and R. C. Martin, Atmospheric methane data for the period 1986-1988 from the NOAA/CMDL global cooperative flask sampling network, Tech. Mem., ERL CMDL-2, NOAA, Boulder, CO., 1990B.
- Lomb, N. R., Least-squares frequency analysis of unequally spaced data, Astrophysics and Space Science, Vol. 39, pp. 447-462, 1976.
- Mayewski, P. A., L. D. Meeker, M. C. Morrison, M. S. Twickler, S. I. Whitlow, K. K. Ferland, D. A. Meese, M. R. Legrand, and J. P. Steffensen, Greenland ice core "signal" characteristics: An expanded view of climate change, J. Geophys. Res., Vol. 98, No. D7, pp. 12,839-12,847, 20 July, 1993.
- McRae J. E. and T. E. Graedel, Carbon Dioxide in the Urban Atmosphere: Dependencies and Trends, J. Geophys. Res., Vol. 84, No. C8, 5011-5017, 20 August 1979.
- Meeker, L. D., P. A. Mayewski, and P. Bloomfield, A new approach to glaciochemical time series analysis, NATO ASI Series, Vol. I 30, 1995.
- Melloh, R. A. and P. M. Crill, Winter methane dynamics in a temperate peatland, Global Biogeo. Cycles, Vol. 10, No. 2, pp. 247-254, June 1996.
- Munger J. W., S. C. Wofsy, P. S. Bakwin, S. Fan, M. L. Goulden, B. C., Daube, and A.H. Goldstein, Atmospheric deposition of reactive nitrogen oxides and ozone in a temperate deciduous forest and a subarctic woodland. 1. Measurements and mechanisms, J. Geophys. Res., Vol. 101, No. D7, 12,639-12,657, 20 May 1996.
- Piccot, S., L. Beck, S. Srinivasan, and S. Kersteter, Global methane emissions from minor anthropogenic sources and biofuel combustion in residential stoves, J. Geophys. Res., Vol. 101, No. D17, pp. 22,757-22,766, 20 October, 1996.
- Shipham, M. C., A. S. Bachmeier, D. R. Cahoon, G. L. Gregory, B. E. Anderson and E. V. Browell, A Meteorological Interpretation of the Arctic Boundary Layer Expedition (ABLE) 3B Flight Series, J. Geophys. Res., Vol 99, No. D1, pp. 1645-1657, 20 January, 1994.
- Sokal, R. R. and F. J. Rohlf, Biometry: The principles and practice of statistics in biological research, W.H. Freeman and Co., New York, 1981.

- Steele L. P., P. J. Fraser, R. A. Rasmussen, M. A. Khalil, T. J. Conway, A. J. Crawford, R. H. Gammon, K. A. Masarie, and K. W. Thoning, The global distribution of methane in the troposphere, J. Atmos. Chem., Vol. 5, pp. 125-171, 1987.
- Steele, L. P., E. J. Dlugokencky, P. M. Lang, P. P. Tans, R. C. Martin, and K. A. Masarie, Slowing down of the global accumulation of atmospheric methane during the 1980's, Nature, Vol. 358, pp. 313-316, 1992.
- Thom M., R. Bosinger, M. Schmidt, and I. Levin, The regional budget of atmospheric methane of a highly populated area, Chemosphere, Vol. 26, Nos. 1-4, pp. 143-160, 1993.
- Thompson, A. M., J. A. Chappellaz, I. Y. Fung, and T. L. Kucsera, The atmospheric CH₄ increase since the last glacial maximum, Tellus, Vol. 45B, pp. 242-257, 1993.
- U. S. Environmental Protection Agency, Anthropogenic methane emissions in the United States: Estimates for 1990, EPA 430-R-93-003, Off. of Air and Radiation, Washington D. C., 1993.
- U. S. Environmental Protection Agency, Inventory of U. S. greenhouse gas emissions and sinks: 1990-1993, EPA 230-R-94-104, Off. of Policy, Planning and Eval., Washington, D. C., 1994.